Title: Twisted bilayers: magic continuum, noncollinear magnetism and more

Speakers: Zhu-Xi Luo

Series: Quantum Matter

Date: November 25, 2021 - 3:30 PM

URL: https://pirsa.org/21110030

Abstract: Van der Waals heterostructures provide a rich venue for exotic moir\'e phenomena. In this talk, I will present a couple of unconventional examples beyond the celebrated twisted bilayer graphene. I will start by twisted bilayer of square lattice with staggered flux, which exhibits a continuum range of magic twisting angles where an exponential reduction of Dirac velocity and bandwidths occurs. Then I will discuss moir\'e magnetism arising from twisted bilayers of antiferromagnets and also ferromagnets. Despite the fact that the parent materials all exhibit collinear orderings, the bilayer system shows controllable emergent noncollinear spin textures. Time permitting, I will also discuss a theory for the potentially continuous metal-insulator transition with fractionalized electric charges in transition metal dichalcogenide moir\'e heterostructures.

Zoom Link: https://pitp.zoom.us/j/99322296758?pwd=WUNGcE1JS3FpZ1VxbklsSCtYTEJVdz09

Twisted bilayers:
Moiré magnetism, magic continuum and more

Zhu-Xi Luo
University of California, Santa Barbara

11/25/2021
PI Virtual Seminar

Simons Collaboration on Ultra-Quantum Matter

UC SANTA BARBARA Quantum Foundry
DMR-1906325

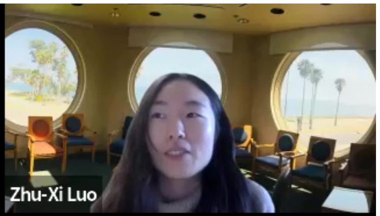

Van der Waals heterostructures

Atomic lego

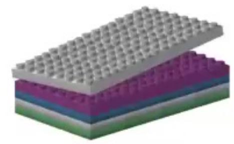

- Two-dimensional atomic crystals
- Highly controllable and tunable
- Stacking with high precision
- Moiré physics
- Example: beats

Van der Waals heterostructures

Atomic lego

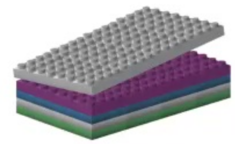

- Two-dimensional atomic crystals
- Highly controllable and tunable
- Stacking with high precision
- Moiré physics
- Example: beats

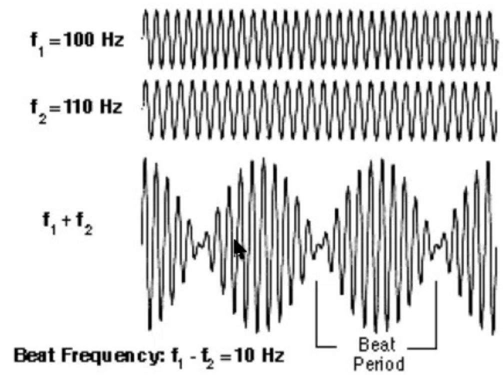

$$\cos(2\pi f_1 t) + \cos(2\pi f_2 t) = 2\cos\left(2\pi \frac{f_1 + f_2}{2} t\right) \cos\left(2\pi \frac{f_1 - f_2}{2} t\right)$$

$$f_{\text{beat}} = f_1 - f_2$$

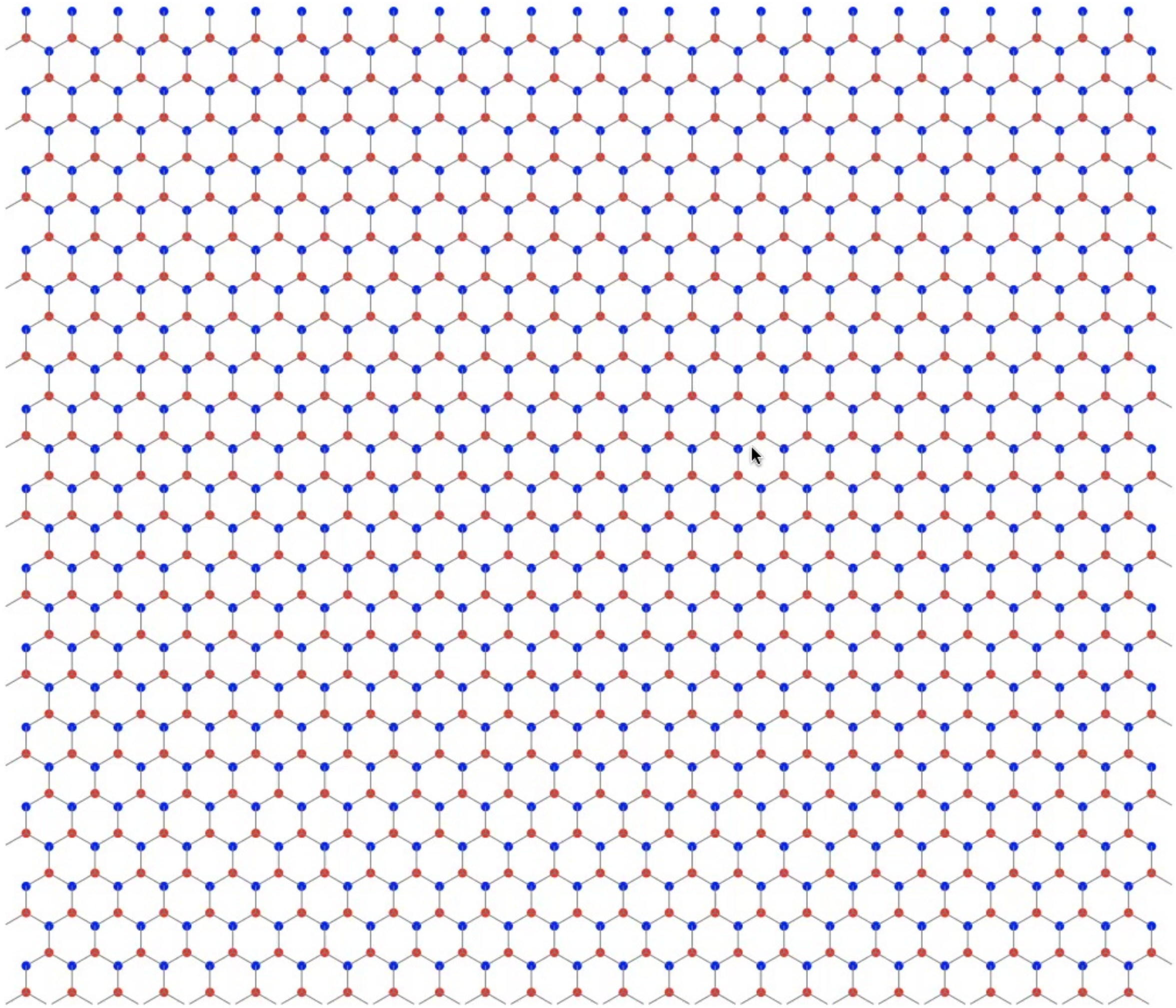


Zhu-Xi Luo

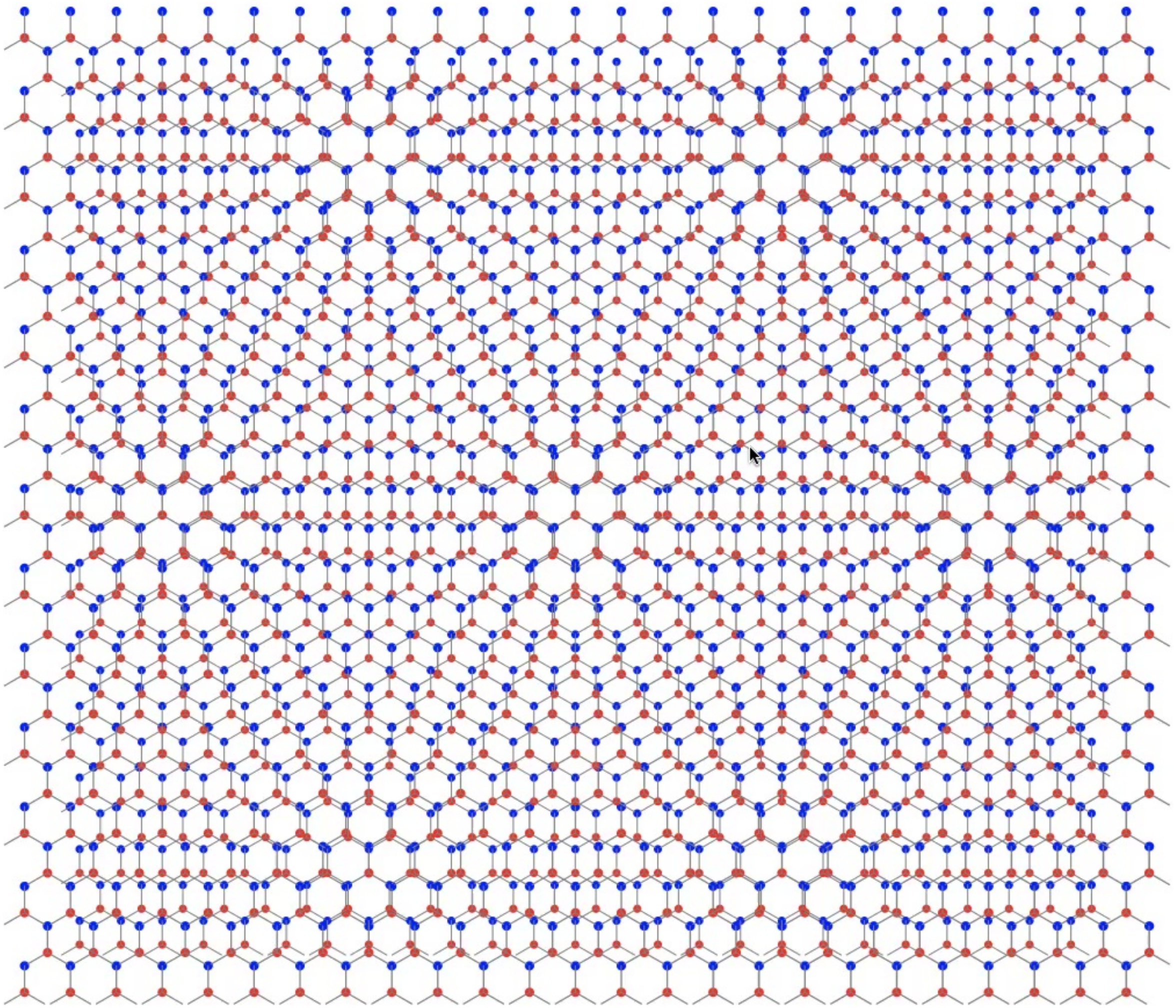


Zhu-Xi Luo

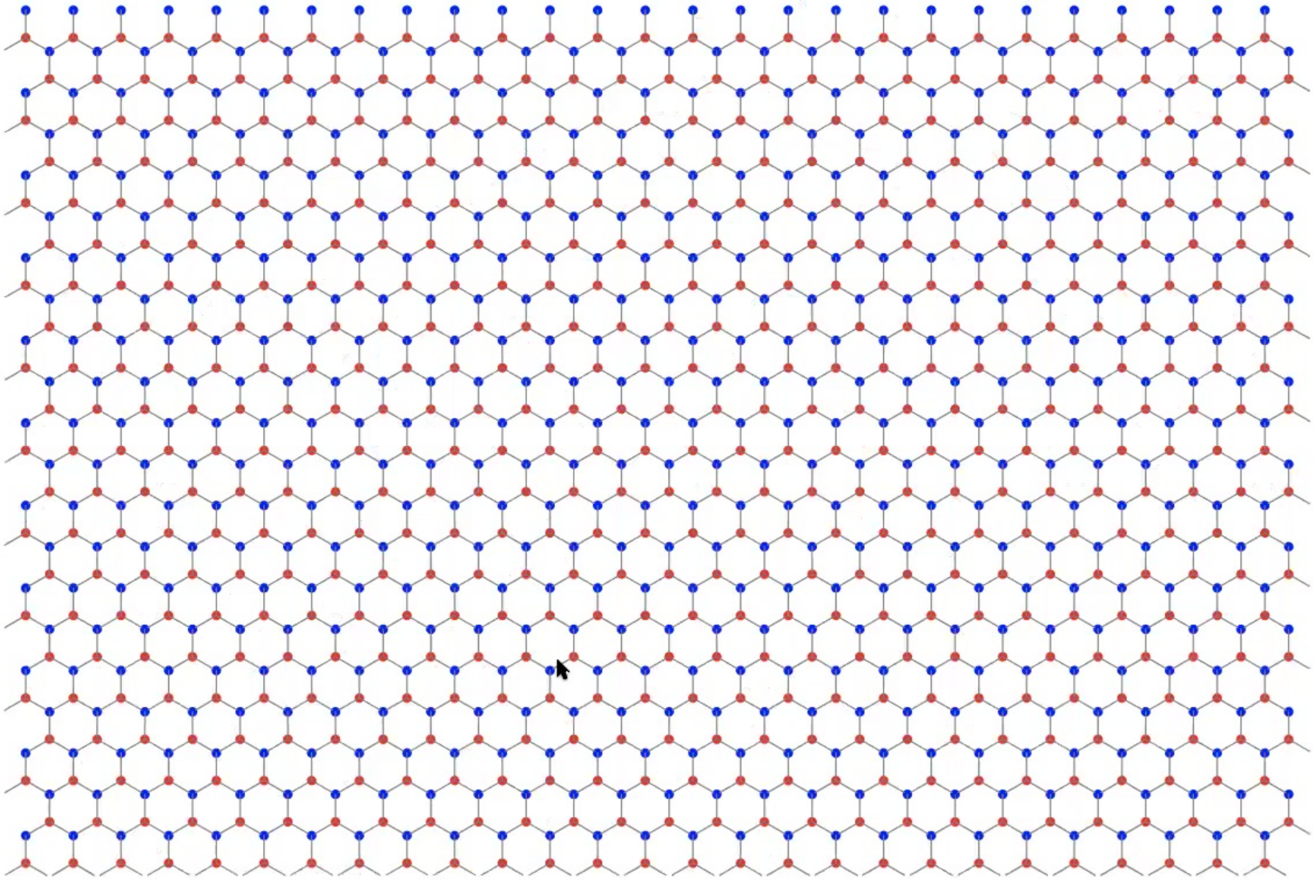

$\theta = 36^\circ$

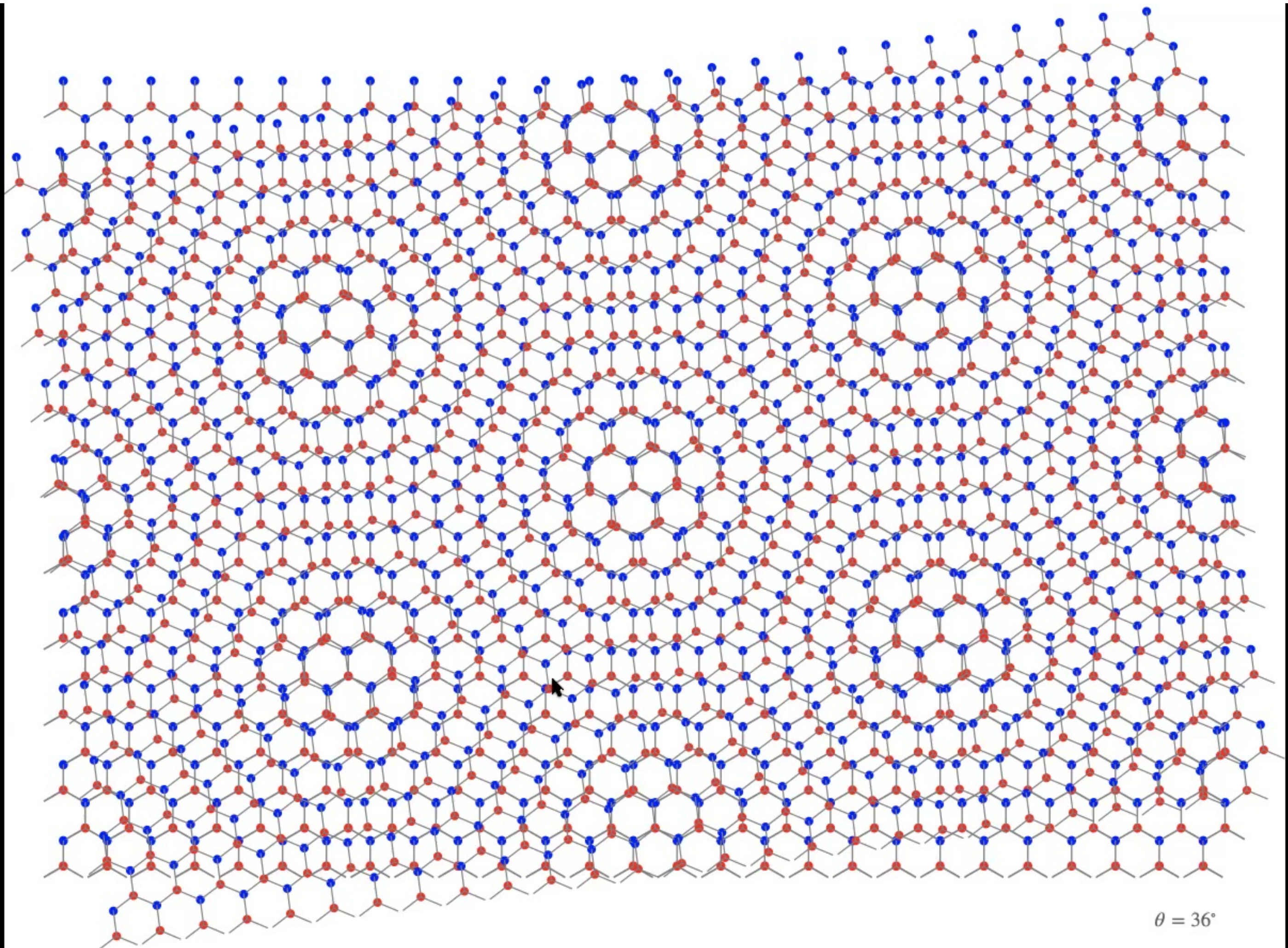
$\theta = 36^{\circ}$


Zhu-Xi Luo

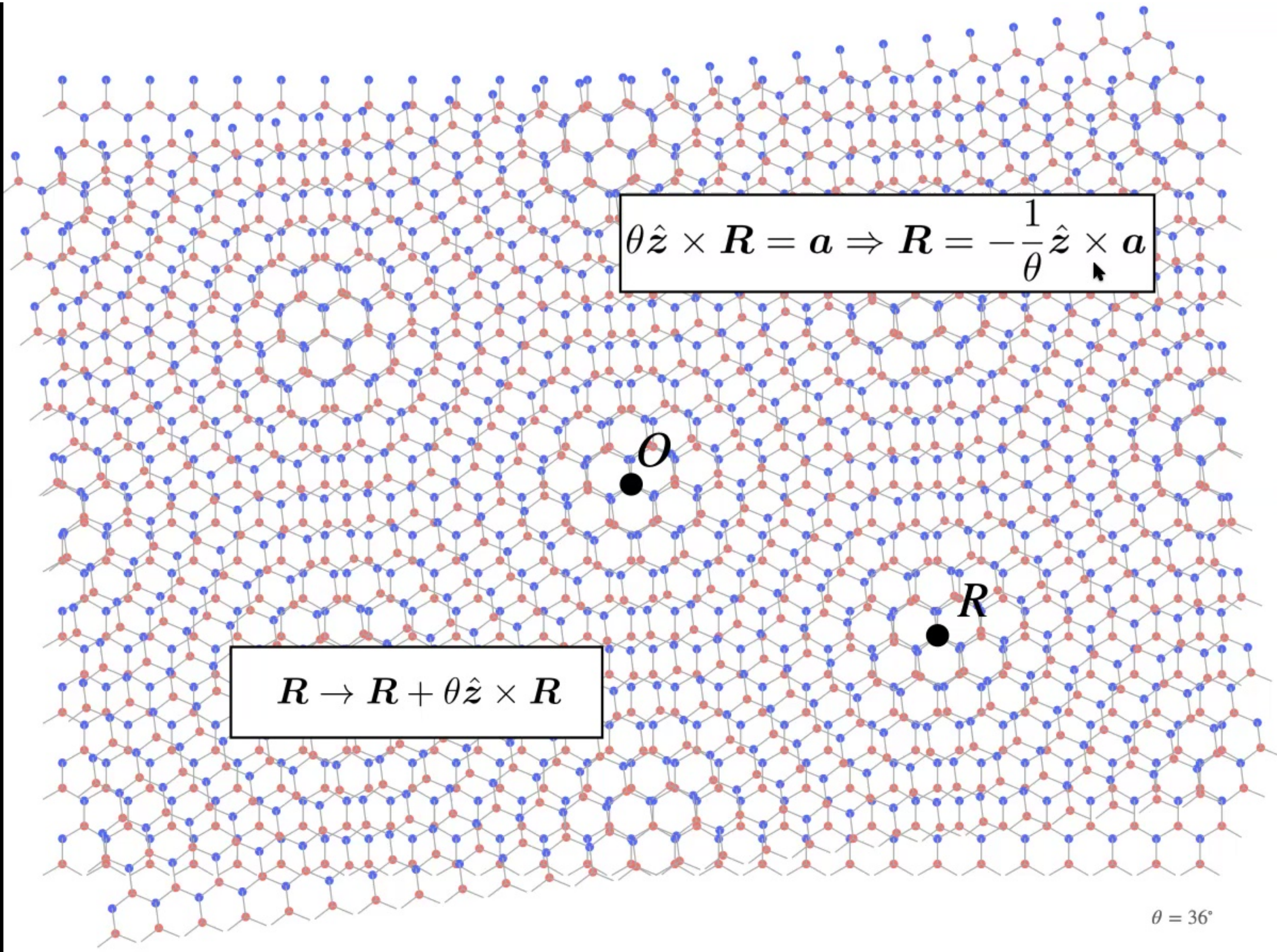

$$\theta \hat{\boldsymbol{z}} \times \boldsymbol{R} = \boldsymbol{a} \Rightarrow \boldsymbol{R} = -\frac{1}{\theta} \hat{\boldsymbol{z}} \times \boldsymbol{a}$$

$$\boldsymbol{R} \to \boldsymbol{R} + \theta \hat{\boldsymbol{z}} \times \boldsymbol{R}$$

Van der Waals heterostructures

Atomic lego

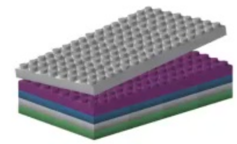

Unconventional superconductivity in magic-angle graphene superlattices

Yuan Cao[1], Valla Fatemi[1], Shiang Fang[2], Kenji Watanabe[3], Takashi Taniguchi[3], Efthimios Kaxiras[2,4] & Pablo Jarillo-Herrero[1]

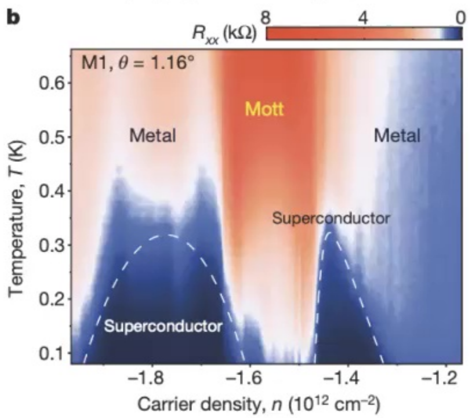

Lego figure: Geim & Grigorieva (2013)

Van der Waals heterostructures

Atomic lego

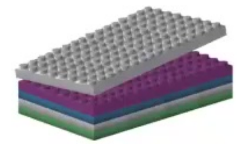

Signatures of tunable superconductivity in a trilayer graphene moiré superlattice

Guorui Chen[1,2,13], Aaron L. Sharpe[3,4,13], Patrick Gallagher[1,2], Ilan T. Rosen[3,4], Eli J. Fox[4,5], Lili Jiang[2], Bosai Lyu[6,7], Hongyuan Li[6,7], Kenji Watanabe[8], Takashi Taniguchi[8], Jeil Jung[9], Zhiwen Shi[6,7], David Goldhaber-Gordon[4,5]*, Yuanbo Zhang[7,10,11]* & Feng Wang[1,2,12]*

Unconventional superconductivity in magic-angle graphene superlattices

Yuan Cao[1], Valla Fatemi[1], Shiang Fang[2], Kenji Watanabe[3], Takashi Taniguchi[3], Efthimios Kaxiras[2,4] & Pablo Jarillo-Herrero[1]

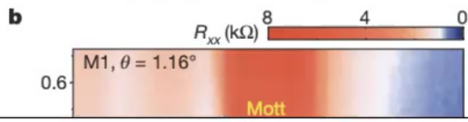

PHYSICAL REVIEW LETTERS 123, 237201 (2019)
Editors' Suggestion

Electronic Properties of α-$RuCl_3$ in Proximity to Graphene

Sananda Biswas[1,*] Ying Li,[1,2] Stephen M. Winter,[1] Johannes Knolle,[3,4,5] and Roser Valentí[1]

TABLE I. Comparison of magnetic interactions in meV for strained α-$RuCl_3$ (see text for description) from current study and unstrained Z-bond of bulk α-$RuCl_3$ in $C/2m$ structure from Ref. [10]. Values are obtained by exact diagonalization on two-site clusters employing $U = 3$ eV, $J_H = 0.6$ eV, $\lambda = 0.15$ eV.

Bond	J	K	Γ	Γ'	$\lvert K/J \rvert$
X, Y	-0.5	-16.8	+1.8	-2.7	33.60
Z	-0.4	-17.2	+1.9	-2.4	43.00
Z ($C2/m$)	-3.0	-7.3	+8.4	-2.0	2.43

Strong interlayer coupling in van der Waals heterostructures built from single-layer chalcogenides

Hui Fang[a,b], Corsin Battaglia[a,b], Carlo Carraro[c], Slavomir Nemsak[d], Burak Ozdol[e,f], Jeong Seuk Kang[a,b], Hans A. Bechtel[g], Sujay B. Desai[a,b], Florian Kronast[h], Ahmet A. Unal[h], Giuseppina Conti[b,d], Catherine Conlon[b,d], Gunnar K. Palsson[b,d], Michael C. Martin[g], Andrew M. Minor[e,f], Charles S. Fadley[b,d], Eli Yablonovitch[a,b,1], Roya Maboudian[c], and Ali Javey[a,b,1]

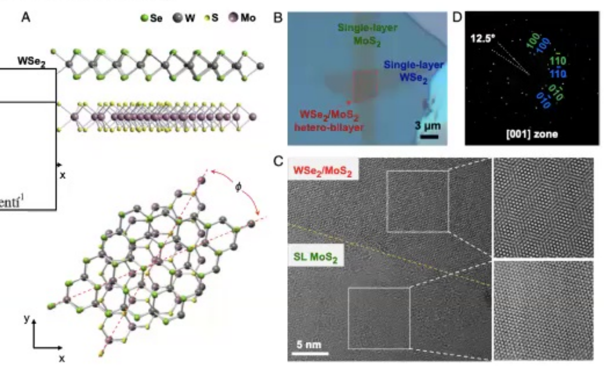

Lego figure: Geim & Grigorieva (2013)

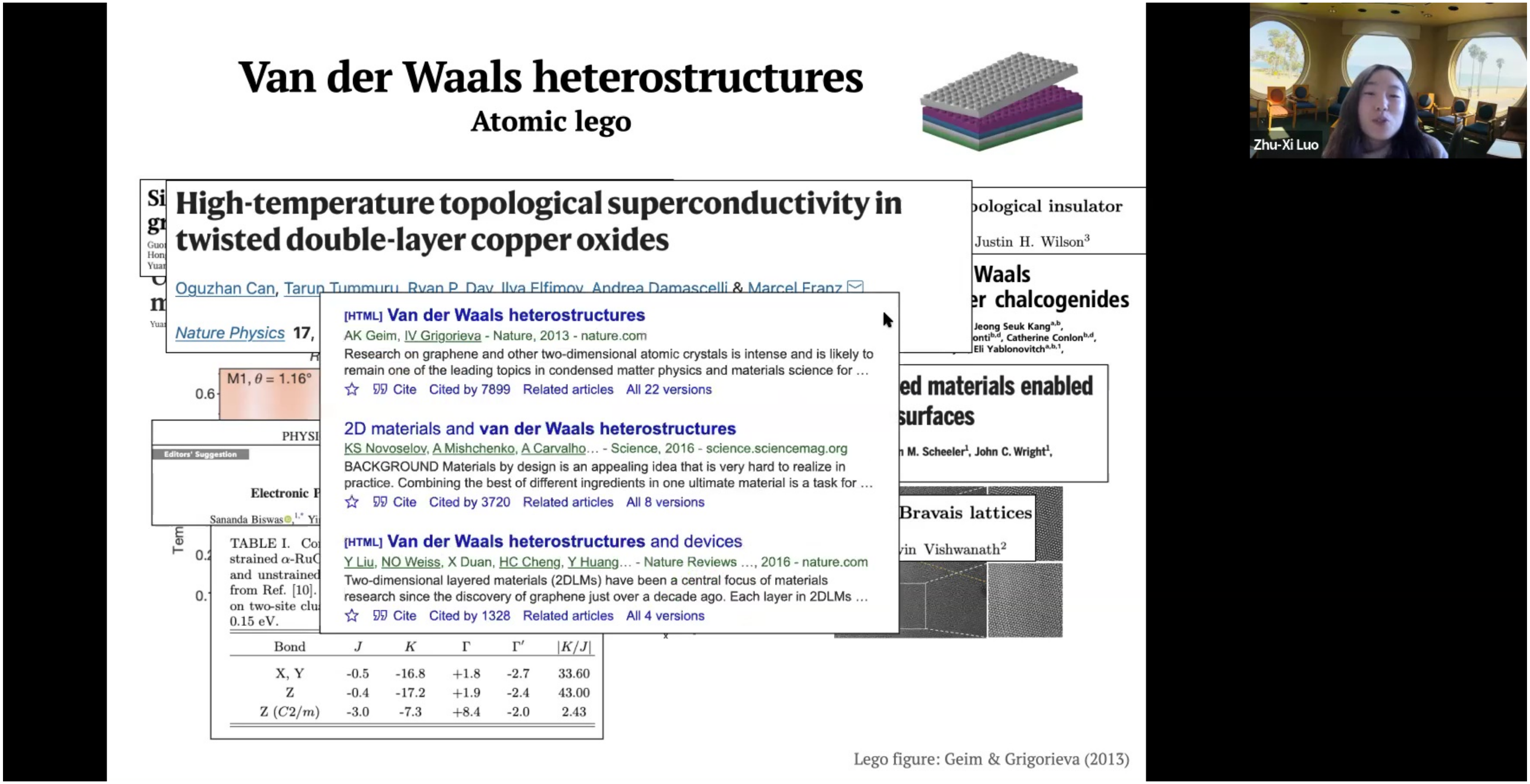
Van der Waals heterostructures
Atomic lego
High-temperature topological superconductivity in twisted double-layer copper oxides
Oguzhan Can, Tarun Tummuru, Ryan P. Day, Ilya Elfimov, Andrea Damascelli & Marcel Franz
Nature Physics 17,
[HTML] Van der Waals heterostructures
AK Geim, IV Grigorieva - Nature, 2013 - nature.com
Research on graphene and other two-dimensional atomic crystals is intense and is likely to remain one of the leading topics in condensed matter physics and materials science for …
Cite Cited by 7899 Related articles All 22 versions
2D materials and van der Waals heterostructures
KS Novoselov, A Mishchenko, A Carvalho… - Science, 2016 - science.sciencemag.org
BACKGROUND Materials by design is an appealing idea that is very hard to realize in practice. Combining the best of different ingredients in one ultimate material is a task for …
Cite Cited by 3720 Related articles All 8 versions
[HTML] Van der Waals heterostructures and devices
Y Liu, NO Weiss, X Duan, HC Cheng, Y Huang… - Nature Reviews …, 2016 - nature.com
Two-dimensional layered materials (2DLMs) have been a central focus of materials research since the discovery of graphene just over a decade ago. Each layer in 2DLMs …
Cite Cited by 1328 Related articles All 4 versions
M1, θ = 1.16°
Editors' Suggestion
Electronic
Sananda Biswas
TABLE I.
Bond | J | K | Γ | Γ′ | |K/J|
X, Y | -0.5 | -16.8 | +1.8 | -2.7 | 33.60
Z | -0.4 | -17.2 | +1.9 | -2.4 | 43.00
Z (C2/m) | -3.0 | -7.3 | +8.4 | -2.0 | 2.43
pological insulator
Justin H. Wilson
Waals
er chalcogenides
ed materials enabled
surfaces
Bravais lattices
vin Vishwanath
Lego figure: Geim & Grigorieva (2013)
Zhu-Xi Luo

What do we do with vdw materials?

A very rough map

What do we do with vdw materials?

A very rough map

What do we do with vdw materials?

A very rough map

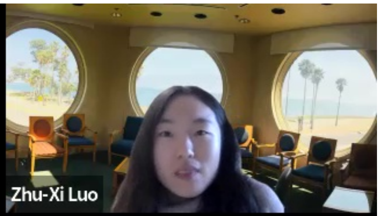

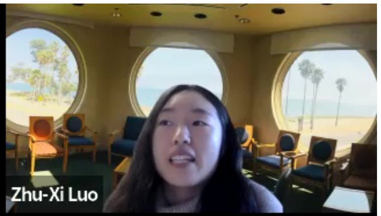

Outline

- A very rough map
- Moiré magnetism
- Magic continuum in TB square lattice
- *Continuous metal-insulator transition
- Outlook

Kasra Hejazi, ZXL and Leon Balents, PNAS (2020) and PRB Lett. (2021)

VdW magnets

- magnetic graphene!

- Can realize fundamental spin Hamiltonians
- Controllable ground states
- Possibility of unconventional magnetism.

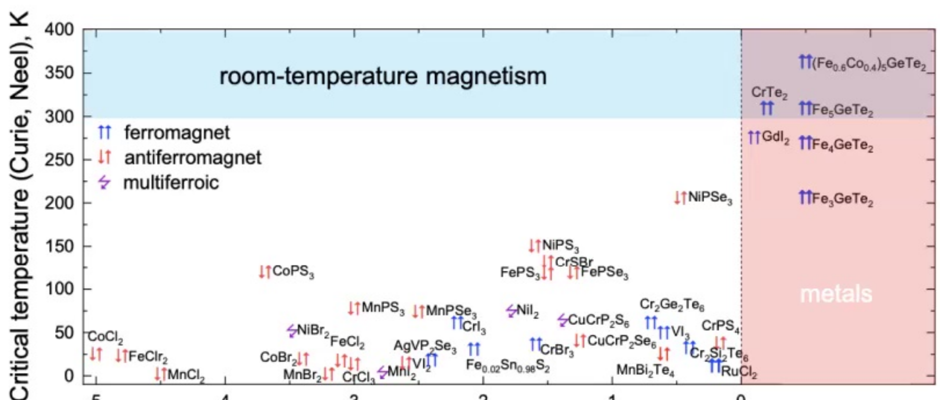

Zoo of materials

Figure credit: I. Verzhbitskiy (2020).

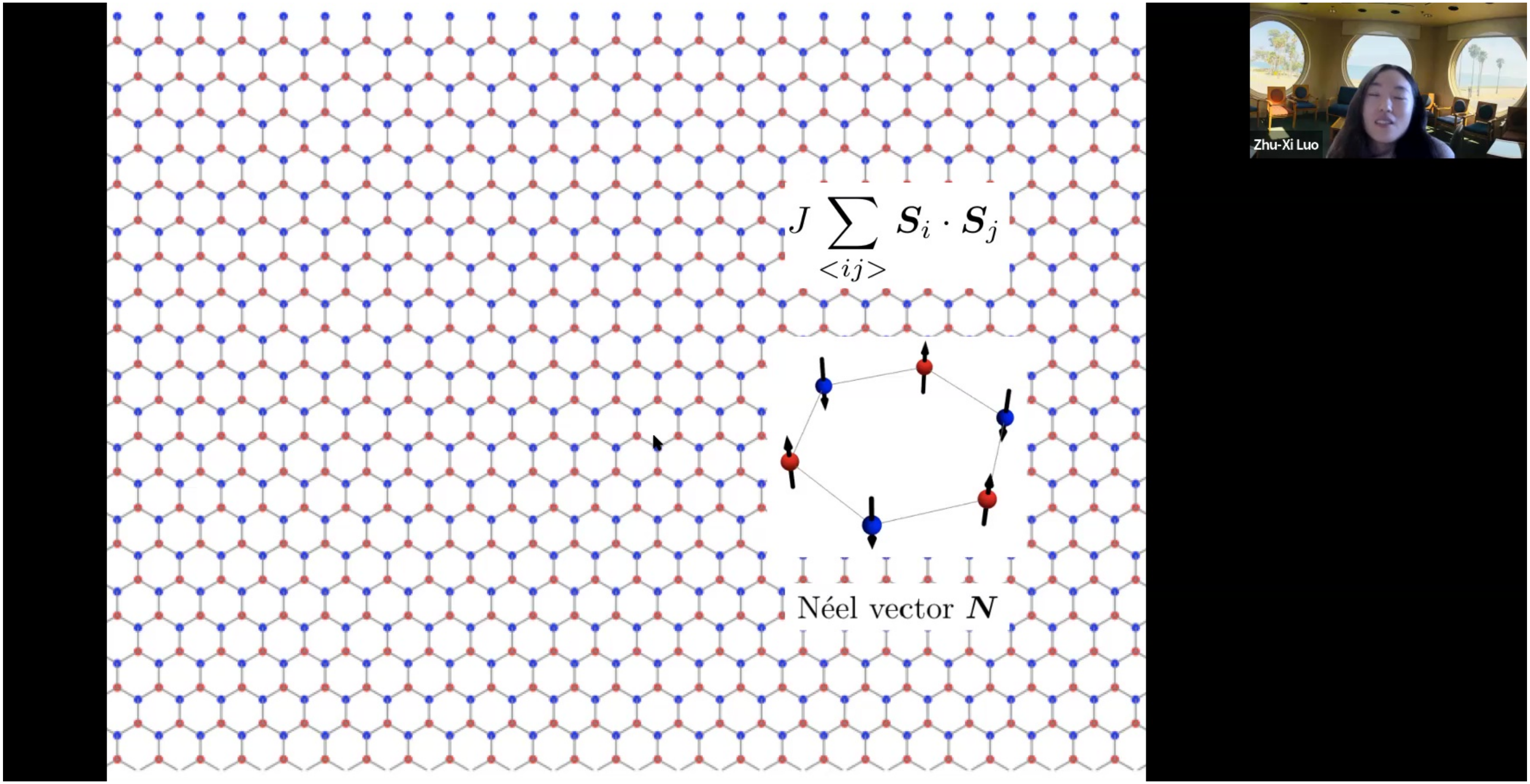
$J \sum_{<ij>} \boldsymbol{S}_i \cdot \boldsymbol{S}_j$
Néel vector $\boldsymbol{N}$
Zhu-Xi Luo

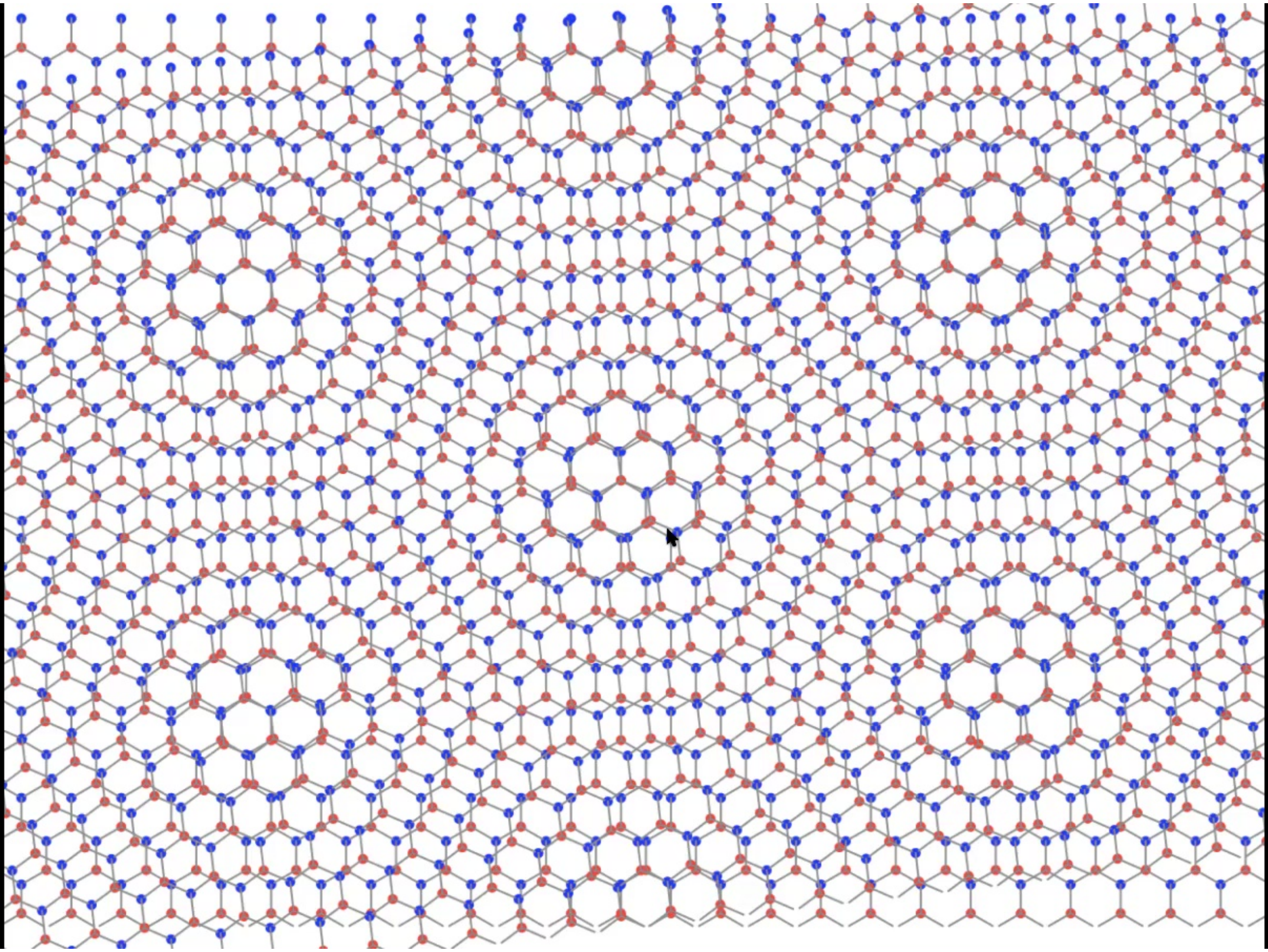

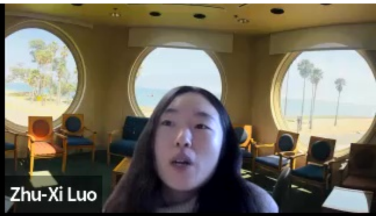
Zhu-Xi Luo

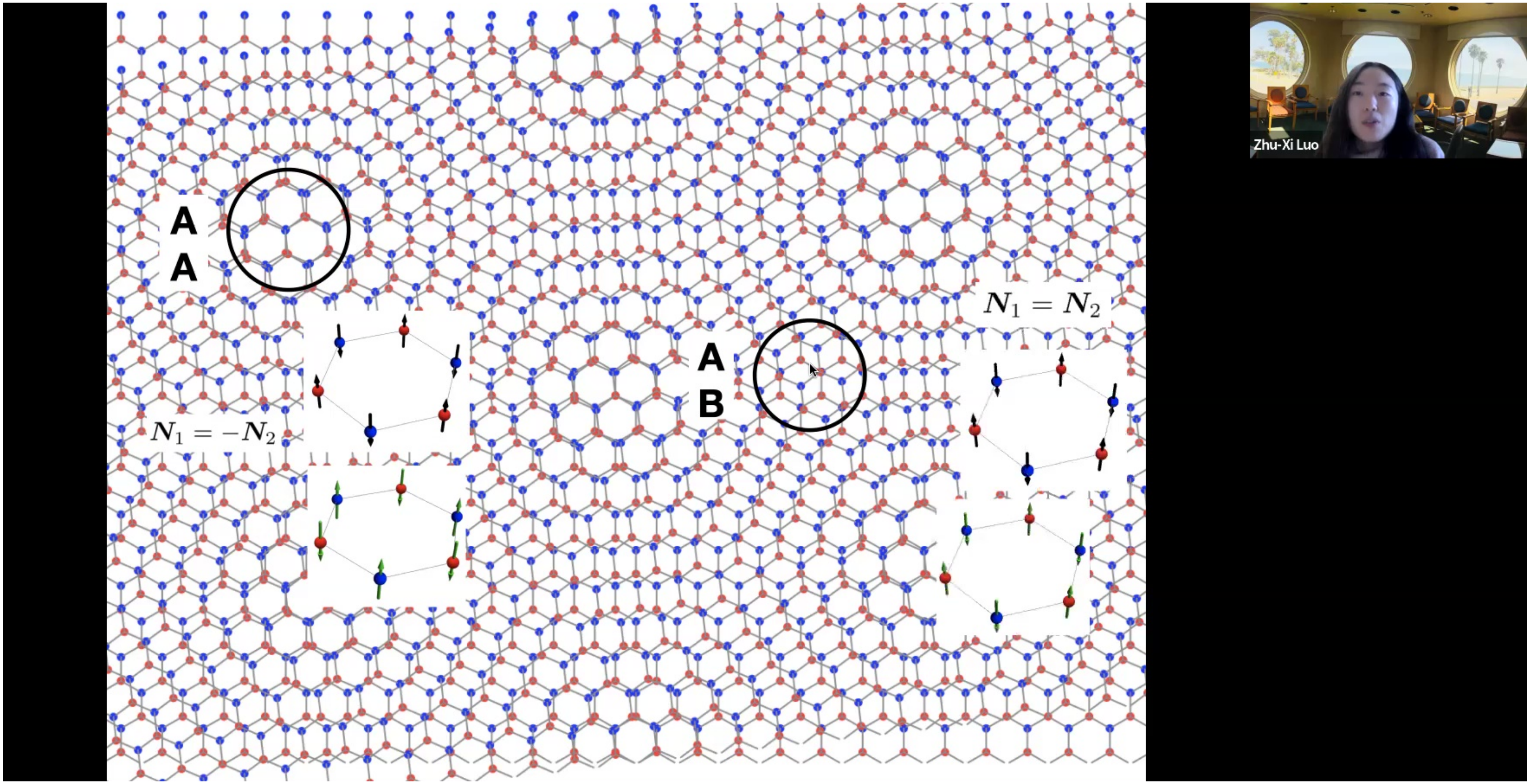
A
A
$N_1 = -N_2$
A
B
$N_1 = N_2$
Zhu-Xi Luo

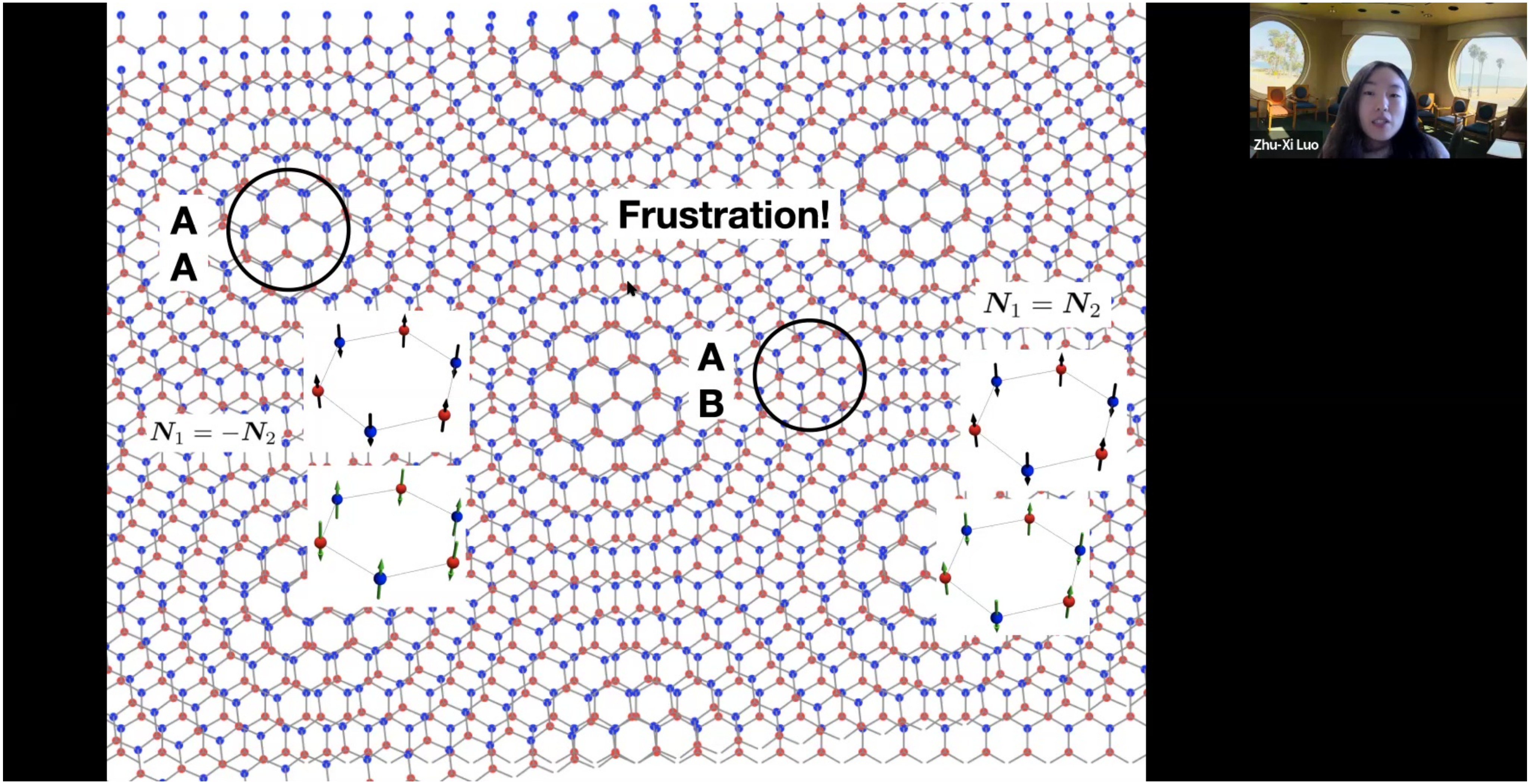
A
A
Frustration!
$N_1 = N_2$
A
B
$N_1 = -N_2$
Zhu-Xi Luo

A continuum formalism

- Simple and elegant

- Restores periodicity, enabling Bloch's theorem
- No need to consider numerous lattice sites with complicated local environments
- Reduces the number of dimensionless parameters

TBG: Bistritzer and MacDonald (2011); Balents (2019)

A continuum formalism

- Simple and elegant

- Restores periodicity, enabling Bloch's theorem
- No need to consider numerous lattice sites with complicated local environments
- Reduces the number of dimensionless parameters
- Works for general elastic deformation. Assumptions:

  - small displacement gradients $\partial_\mu u \ll 1$

  - small interlayer exchange $J' \ll J$

TBG: Bistritzer and MacDonald (2011); Balents (2019)

General formalism

- Eulerian coordinates $\boldsymbol{x} = \boldsymbol{R} + \boldsymbol{u}(\boldsymbol{x})$

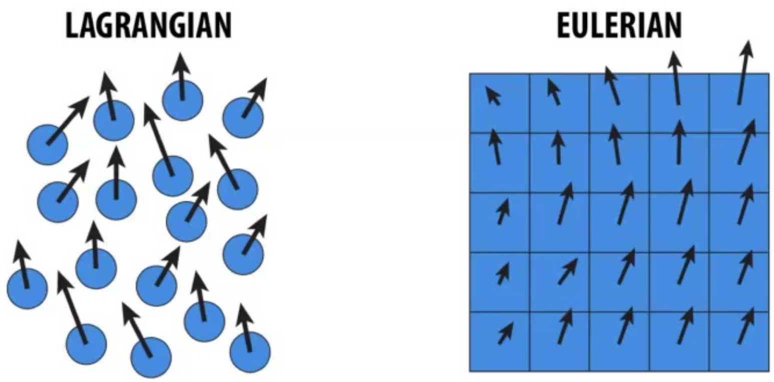

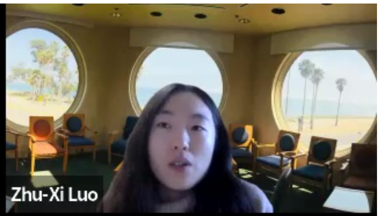

General formalism

- Single layer: AFM Heisenberg model

$$\mathcal{L}_0[\boldsymbol{N}_l] = \frac{\rho}{2v^2}\left(\partial_t \boldsymbol{N}_l\right)^2 - \frac{\rho}{2}\left(\nabla \boldsymbol{N}_l\right)^2 + d\left(N_l^z\right)^2$$

- Displacement effect:

$$\mathcal{L}_1[\mathbf{N}_l, \mathbf{u}_l] = \rho(\varepsilon_{l,xx}+\varepsilon_{l,yy})\left[\frac{\delta_1}{v^2}\left(\partial_t \mathbf{N}_l\right)^2 - \delta_2\left(\nabla \mathbf{N}_l\right)^2\right] + \delta_3 \varepsilon_{l,\mu\nu}\partial_\mu \mathbf{N}_l \cdot \partial_\nu \mathbf{N}_l$$

- Interlayer term based on locality and translation symmetry:

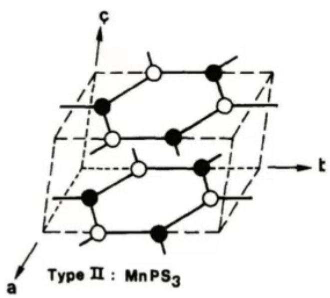

R. Brev, Solid State Ionics 1986, 22, 3

General formalism

- Single layer: AFM Heisenberg model

$$\mathcal{L}_0[\boldsymbol{N}_l] = \frac{\rho}{2v^2}\left(\partial_t \boldsymbol{N}_l\right)^2 - \frac{\rho}{2}\left(\nabla \boldsymbol{N}_l\right)^2 + d\left(N_l^z\right)^2$$

- Displacement effect:

$$\mathcal{L}_1[\mathbf{N}_l, \mathbf{u}_l] = \rho(\varepsilon_{l,xx} + \varepsilon_{l,yy})\left[\frac{\delta_1}{v^2}\left(\partial_t \mathbf{N}_l\right)^2 - \delta_2\left(\nabla \mathbf{N}_l\right)^2\right] + \delta_3 \varepsilon_{l,\mu\nu}\partial_\mu \mathbf{N}_l \cdot \partial_\nu \mathbf{N}_l$$

- Interlayer term based on locality and translation symmetry:

$$\mathcal{L}_2[\boldsymbol{N}_1, \boldsymbol{N}_2, \boldsymbol{u}_1 - \boldsymbol{u}_2] = J' \; f[\boldsymbol{u}_1 - \boldsymbol{u}_2] \; \boldsymbol{N}_1 \cdot \boldsymbol{N}_2$$

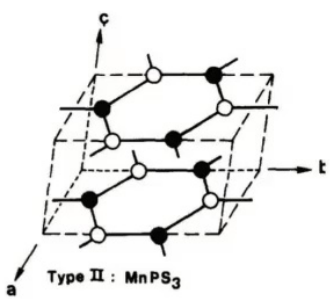

R. Brev, Solid State Ionics 1986, 22, 3

Interlayer term

- Minimal Fourier expansion

$$\mathcal{S}_l(\boldsymbol{x}) = n_0 \boldsymbol{N}_l \sum_{i=1}^{3} \sin(\boldsymbol{b}_i \cdot \boldsymbol{R}) = n_0 \boldsymbol{N}_l \sum_{i=1}^{3} \sin[\boldsymbol{b}_i \cdot (\boldsymbol{x} - \boldsymbol{u}_l)]$$

- The interlayer Heisenberg coupling

$$J' \mathcal{S}_1 \cdot \mathcal{S}_2 \sim J' \sum_{i=1}^{3} \cos(\boldsymbol{b}_i \cdot \boldsymbol{u}(\boldsymbol{x}))$$

- Rigid twist

$$J' \Phi(\boldsymbol{x}) = J' \sum_{i=1}^{3} \cos(\boldsymbol{q}_i \cdot \boldsymbol{x}), \quad \boldsymbol{q}_i = \theta \hat{\boldsymbol{z}} \times \boldsymbol{b}_i$$

- Dimensionless coordinates

$$\mathcal{H} = \sum_l [(\boldsymbol{\nabla} N_l)^2 - \beta (N_l^z)^2] - \alpha \Phi(\boldsymbol{X}) \boldsymbol{N}_1 \cdot \boldsymbol{N}_2$$

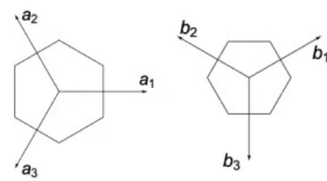

Isotropic case

$$\mathcal{H} = \sum_l [(\nabla N_l)^2 - \beta (N_l^z)^2] - \alpha \Phi(\boldsymbol{X}) \boldsymbol{N}_1 \cdot \boldsymbol{N}_2$$

$$\boldsymbol{N}_l^{cl} = \sin\phi_l \hat{\boldsymbol{x}} + \cos\phi_l \hat{\boldsymbol{z}}$$

$$\mathcal{H} = |\nabla\phi_1|^2 + |\nabla\phi_2|^2 - \alpha\Phi(\boldsymbol{X})\cos(\phi_1 - \phi_2)$$

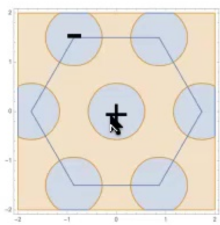

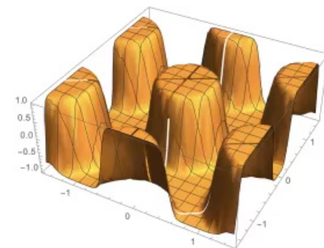

- Large α: parallel or antiparallel depending on the sign of $\Phi(\boldsymbol{X})$
- Small α: perpendicular.
- Three Goldstone modes and flattening of magnon bands at large α.

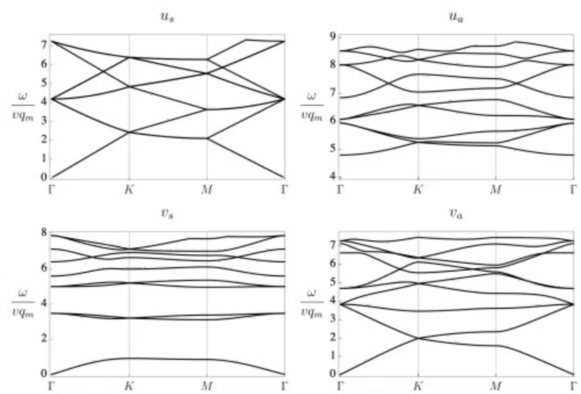

Isotropic case

$$\mathcal{H} = \sum_l [(\nabla N_l)^2 - \beta(N_l^z)^2] - \alpha\Phi(\boldsymbol{X})\boldsymbol{N}_1 \cdot \boldsymbol{N}_2$$

$$\boldsymbol{N}_l^{cl} = \sin\phi_l \hat{\boldsymbol{x}} + \cos\phi_l \hat{\boldsymbol{z}}$$

$$\mathcal{H} = |\nabla\phi_1|^2 + |\nabla\phi_2|^2 - \alpha\Phi(\boldsymbol{X})\cos(\phi_1 - \phi_2)$$

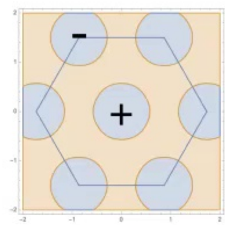

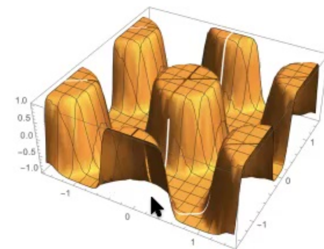

- Large α: parallel or antiparallel depending on the sign of $\Phi(\boldsymbol{X})$
- Small α: perpendicular.
- Three Goldstone modes and flattening of magnon bands at large α.

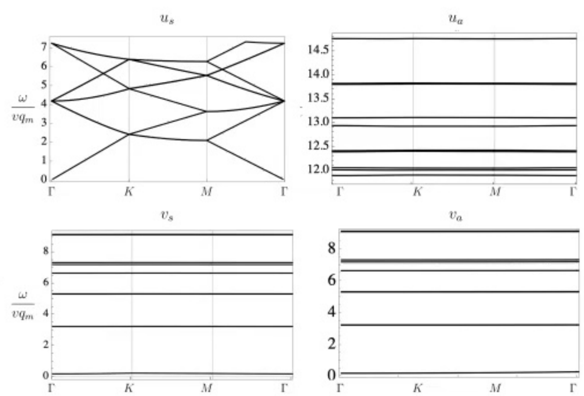

Single-ion anisotropy

$$\mathcal{H} = \sum_l [(\nabla N_l)^2 - \beta (N_l^z)^2] - \alpha \Phi(\boldsymbol{X}) \boldsymbol{N}_1 \cdot \boldsymbol{N}_2$$

Twisted-a

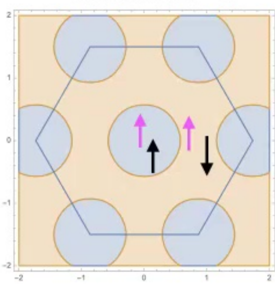

$\phi_s = \phi_a = 0$ or π

Twisted-s

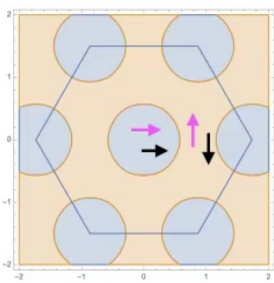

$\phi_s = \pi, \quad \phi_a = 0$ or π

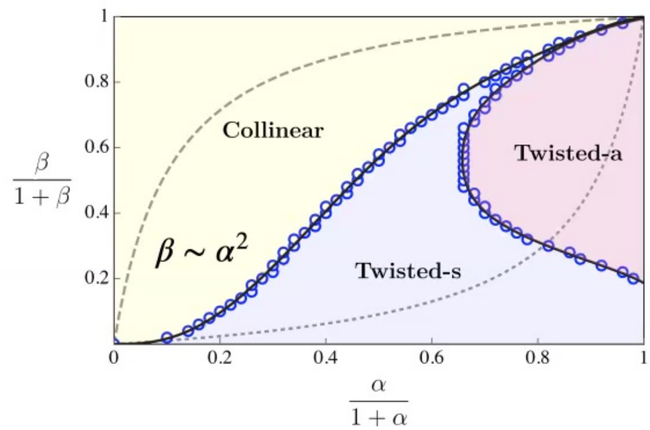

Single-ion anisotropy

$$\mathcal{H} = \sum_l [(\nabla N_l)^2 - \beta (N_l^z)^2] - \alpha \Phi(\boldsymbol{X}) \boldsymbol{N}_1 \cdot \boldsymbol{N}_2$$

$$\mathcal{H}^{cl} = \frac{1}{2}(|\nabla \phi_s|^2 + |\nabla \phi_a|^2) - (\alpha \Phi(\boldsymbol{X}) + \beta \cos \phi_s) \cos \phi_a$$

$$\phi_s = \phi_1 + \phi_2, \quad \phi_a = \phi_1 - \phi_2$$

Twisted-a

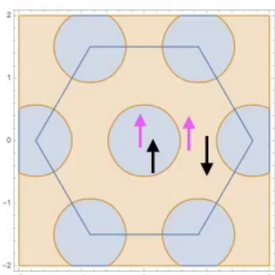

$\phi_s = \phi_a = 0$ or π

Twisted-s

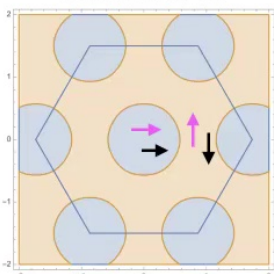

$\phi_s = \pi, \quad \phi_a = 0$ or π

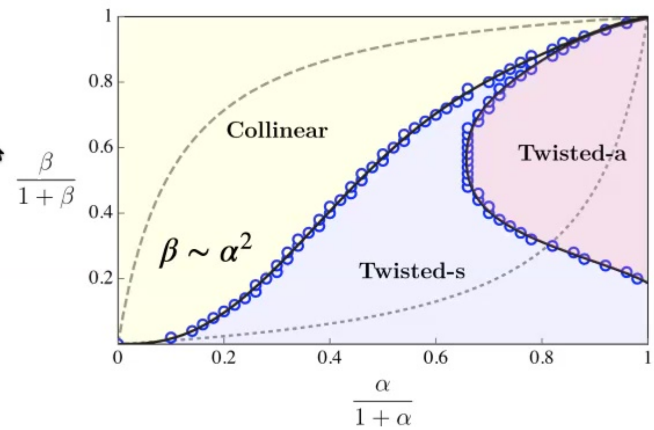

Other examples

CoPS3, NiPS3

FePS3

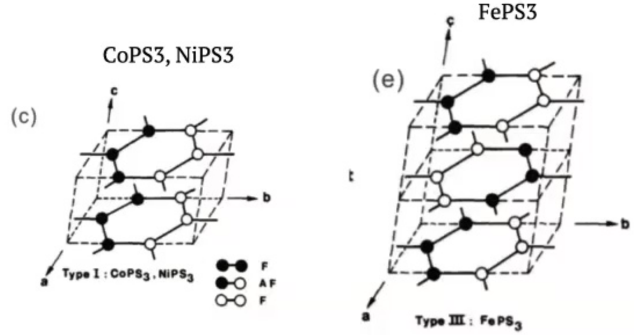

R. Brev, (1986).

Zig-zag AFM

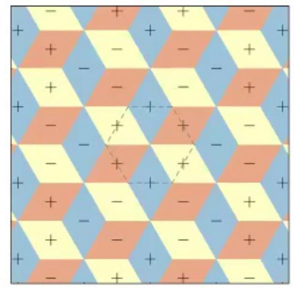

Other examples

CoPS3, NiPS3

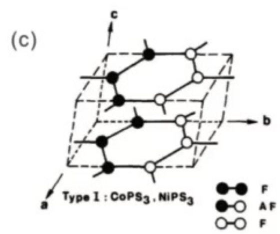

FePS3

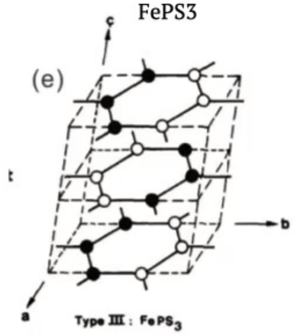

R. Brev, (1986).

Zig-zag AFM

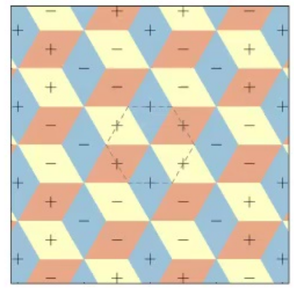

FM: CrI3

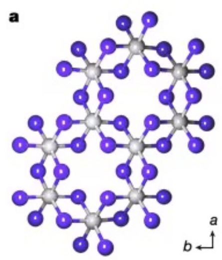

Dillon et al, (1965) & (1966).

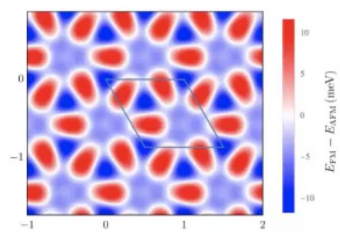

Plotted using data from
Sivadas et al, Nano letters (2018)

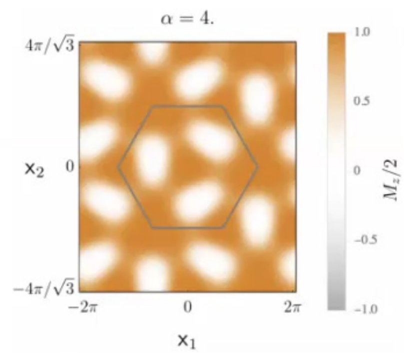

Emergence of a noncollinear magnetic state in twisted bilayer CrI_3

Yang Xu[1,2], Ariana Ray[1], Yu-Tsun Shao[1], Shengwei Jiang[1], Daniel Weber[3], Joshua E. Goldberger[3], Kenji Watanabe[4], Takashi Taniguchi[4], David A. Muller[1,5], Kin Fai Mak[1,5,6*], Jie Shan[1,5,6*]

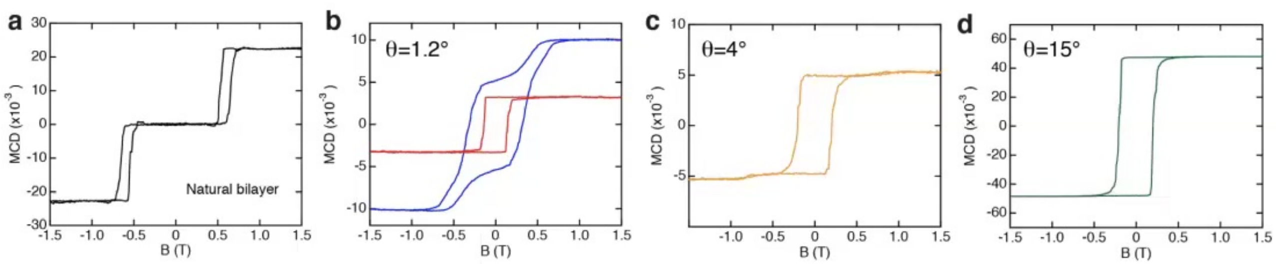

Natural bilayer
AFM

Small twisting
mixture
Large α

Large twisting
FM
Small α

Magnetic skyrmions in vdW magnets

Monolayers

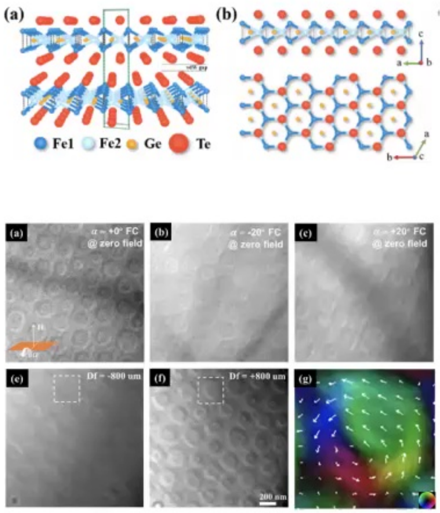

Fe3GeTe2

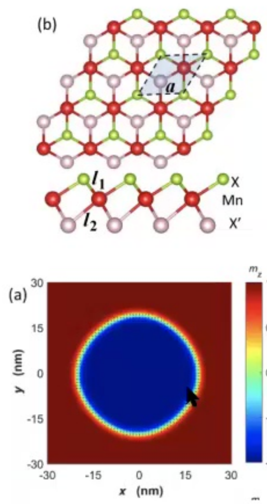

Janus materials

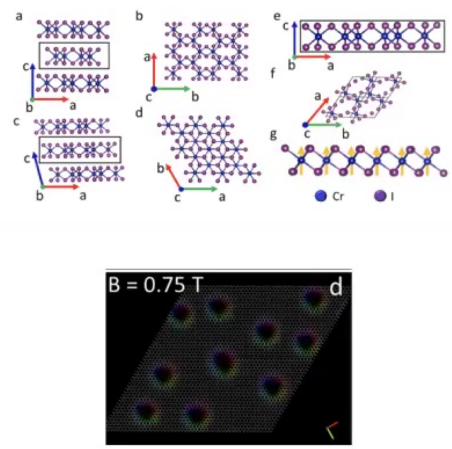

Chromium Iodide

CrI3: Behera et al, Appl. Phys. Lett. 114, 232402 (2019).
Janus: Yuan et al, Phys. Rev. B **101**, 094420 (2020).
FGT: Wang et al, 1907.08382 (2019);
Park et al, 1907.01425 (2019);
Ding et al, Nano Letters 20, 868 (2019)

General formalism

- Single layer: AFM Heisenberg model

$$\mathcal{L}_0[\boldsymbol{N}_l] = \frac{\rho}{2v^2}\left(\partial_t \boldsymbol{N}_l\right)^2 - \frac{\rho}{2}\left(\nabla \boldsymbol{N}_l\right)^2 + d\left(N_l^z\right)^2$$

- Displacement effect:

$$\mathcal{L}_1[\mathbf{N}_l, \mathbf{u}_l] = \rho(\varepsilon_{l,xx} + \varepsilon_{l,yy})\left[\frac{\delta_1}{v^2}\left(\partial_t \mathbf{N}_l\right)^2 - \delta_2\left(\nabla \mathbf{N}_l\right)^2\right] + \delta_3 \varepsilon_{l,\mu\nu}\partial_\mu \mathbf{N}_l \cdot \partial_\nu \mathbf{N}_l$$

- Interlayer term based on locality and translation symmetry:

$$\mathcal{L}_2[\boldsymbol{N}_1, \boldsymbol{N}_2, \boldsymbol{u}_1 - \boldsymbol{u}_2] = J' \; f[\boldsymbol{u}_1 - \boldsymbol{u}_2] \; \boldsymbol{N}_1 \cdot \boldsymbol{N}_2$$

$$\mathcal{L} = \sum_{l=1,2}\left(\mathcal{L}_0[\boldsymbol{N}_l] + \mathcal{L}_1[\boldsymbol{N}_l, \boldsymbol{u}_l]\right) + \mathcal{L}_2[\boldsymbol{N}_1, \boldsymbol{N}_2, \boldsymbol{u}_1 - \boldsymbol{u}_2]$$

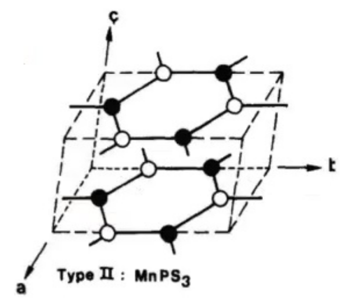

R. Brev, Solid State Ionics 1986, 22, 3

Magnetic skyrmions in vdW magnets

Monolayers

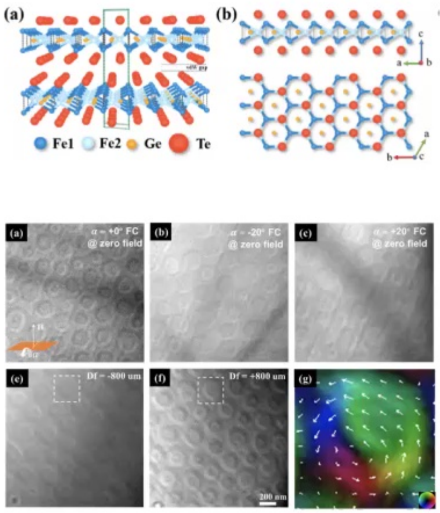

Fe3GeTe2

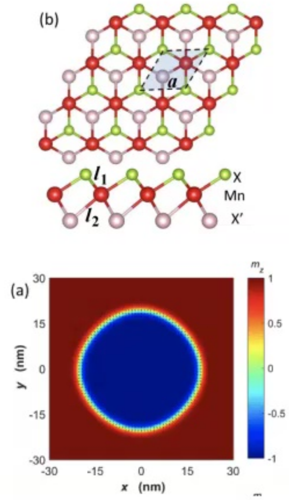

Janus materials

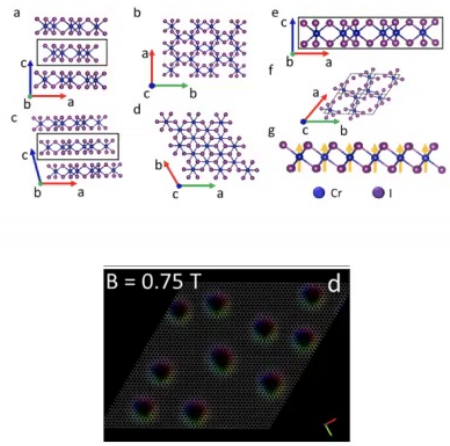

Chromium Iodide

CrI3: Behera et al, Appl. Phys. Lett. 114, 232402 (2019).
Janus: Yuan et al, Phys. Rev. B **101**, 094420 (2020).
FGT: Wang et al, 1907.08382 (2019);
Park et al, 1907.01425 (2019);
Ding et al, Nano Letters 20, 868 (2019)

Moiré skyrmions

in untwisted heterobilayer van der Waals magnets

- DM interaction in the FM layer and anisotropy in AFM

$$\mathcal{H}_0 = \frac{\rho_1}{2}(\nabla \boldsymbol{M})^2 + \frac{\rho_2}{2}(\nabla \boldsymbol{N})^2 + D\boldsymbol{M} \cdot (\nabla \times \boldsymbol{M}) - C(N_z)^2$$

- Small mismatch

$$\mathcal{H}' = J' \boldsymbol{\mathcal{S}}_1 \cdot \boldsymbol{\mathcal{S}}_2 \sim J' \boldsymbol{M} \cdot \boldsymbol{N} \sum_i \sin(\boldsymbol{d}_i \cdot \boldsymbol{r})$$

- Effective Hamiltonian for the AFM layer

$$\mathcal{H} = \frac{1}{2}(\nabla \boldsymbol{M})^2 + \beta \boldsymbol{M} \cdot (\nabla \times \boldsymbol{M}) + \alpha M_z \Phi(\boldsymbol{x})$$

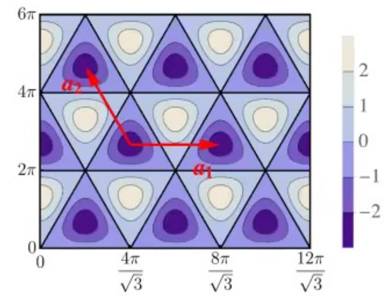

$$\Phi(\boldsymbol{x}) = \sum_i \sin(\boldsymbol{d}_i \cdot \boldsymbol{x})$$

Different limits

$$\mathcal{H} = \frac{1}{2}(\nabla \boldsymbol{M})^2 + \beta \boldsymbol{M} \cdot (\nabla \times \boldsymbol{M}) + \alpha M_z \Phi(\boldsymbol{x})$$

- When $\alpha = 0$, spirals of period $2\pi/\beta$ Moriya (1976).
- $\beta = 0,\ \alpha$ large: coplanar twisted solution with SO(2) symmetry

$$\boldsymbol{M} = (\cos qy, 0, \sin qy)$$

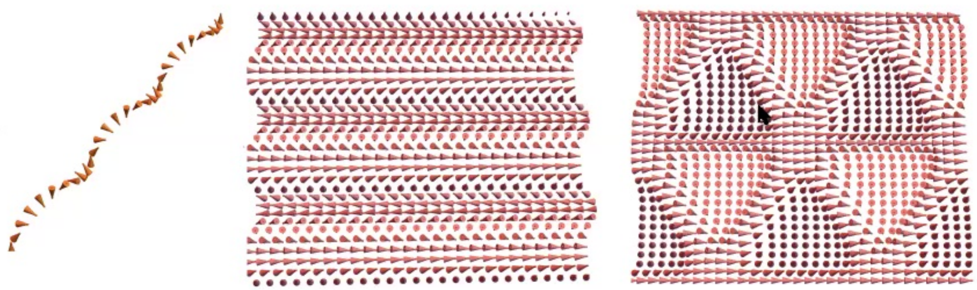

Different limits

$$\mathcal{H} = \frac{1}{2}(\nabla \boldsymbol{M})^2 + \beta \boldsymbol{M} \cdot (\nabla \times \boldsymbol{M}) + \alpha M_z \Phi(\boldsymbol{x})$$

$$= -2\beta \boldsymbol{M} \cdot (\hat{\boldsymbol{z}} \times \boldsymbol{\nabla} M_z) = 2M_z(\partial_x M_y - \partial_y M_z)$$

- When $\alpha = 0$, spirals of period $2\pi/\beta$ Moriya (1976).
- $\beta = 0,\ \alpha$ large: coplanar twisted solution with SO(2) symmetry

$$\boldsymbol{M} = (\cos qy, 0, \sin qy)$$

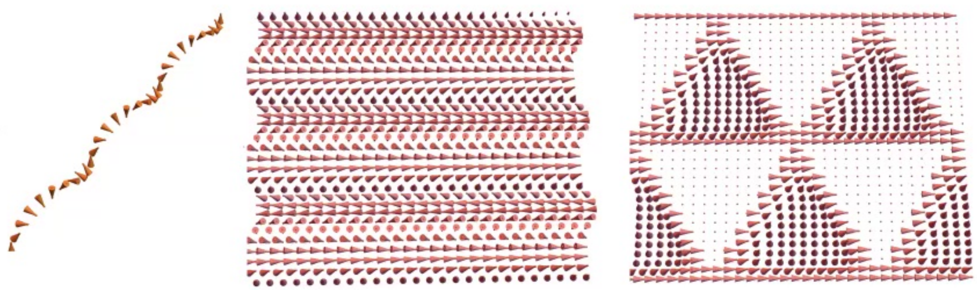

Different limits

$$\mathcal{H} = \frac{1}{2}(\nabla \boldsymbol{M})^2 + \beta \boldsymbol{M} \cdot (\nabla \times \boldsymbol{M}) + \alpha M_z \Phi(\boldsymbol{x})$$

$$= -2\beta \boldsymbol{M} \cdot (\hat{\boldsymbol{z}} \times \boldsymbol{\nabla} M_z) = 2M_z(\partial_x M_y - \partial_y M_z)$$

- When $\alpha = 0$, spirals of period $2\pi/\beta$ Moriya (1976).
- $\beta = 0,\ \alpha$ large: coplanar twisted solution with SO(2) symmetry

$$\boldsymbol{M} = (\cos qy, 0, \sin qy)$$

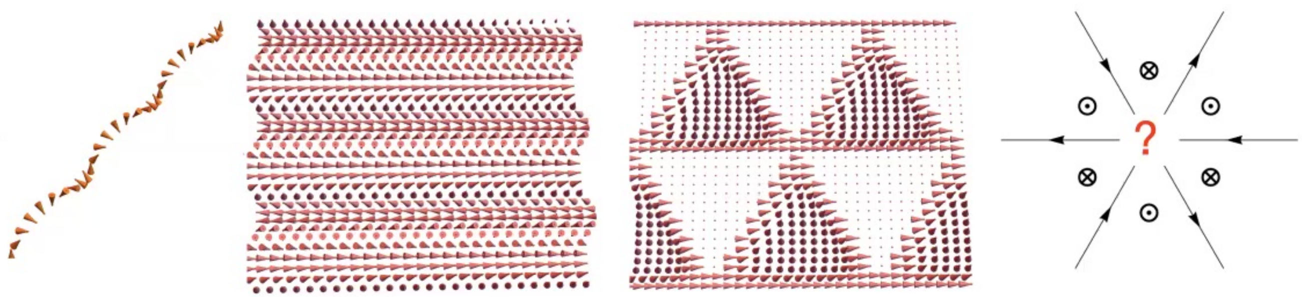

Commensurate configurations

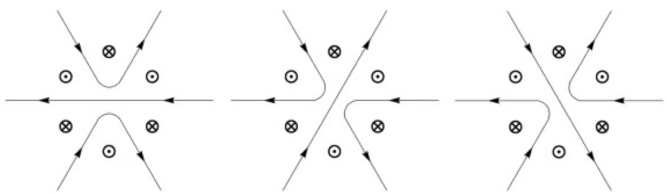

3-state clock vertex

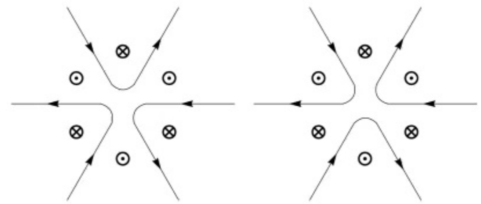

Ising vertex

Commensurate configurations

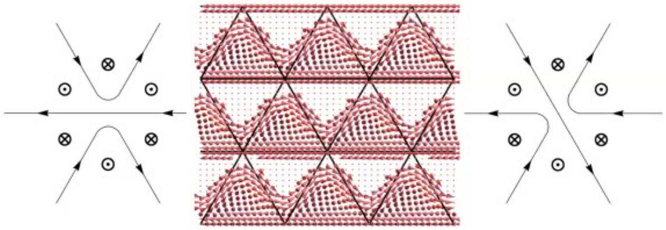

3-state clock vertex

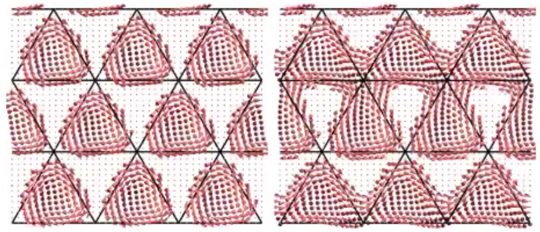

Ising vertex

Commensurate configurations

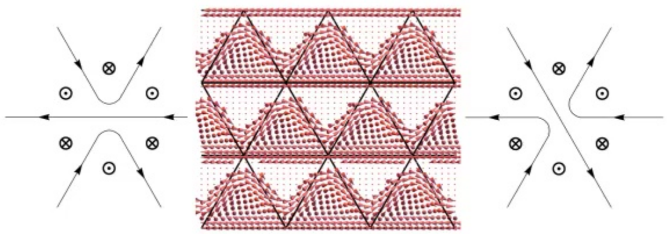

3-state clock vertex

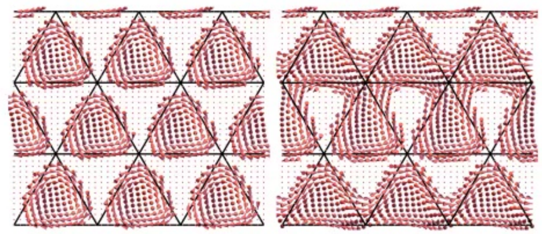

Ising vertex

Numerical minimization

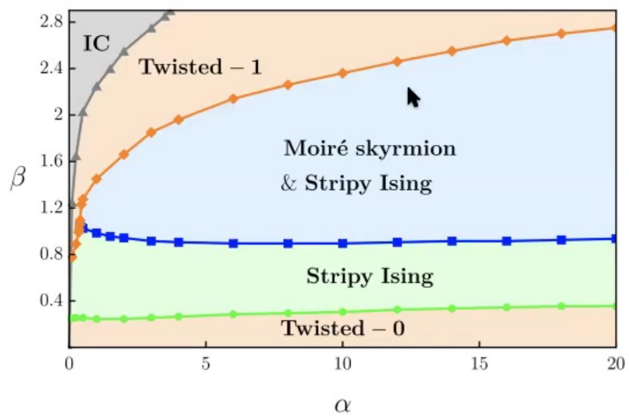

Commensurate-Incommensurate transition

- Weak-coupling analysis

$$\boldsymbol{M} = (\sin\theta\cos\phi, \sin\theta\sin\phi, \cos\theta)$$

- To zeroth order in β, EoM: $\nabla^2\theta + \alpha\sin\theta\,\Phi(\boldsymbol{x}) = \lambda$
- In the commensurate phase, $\bar{\theta} = \pi/2$
- Add slow fluctuations to describe the CI transition.

$$\mathcal{H}^{\text{eff}} = \frac{1}{2}[(\partial_y\bar{\theta} - \beta)^2 + \frac{3}{4}\alpha^2(1-\cos 2\bar{\theta})]$$

FVdM model!

- Soliton solution where $\bar{\theta}$ jumps by π: $\bar{\theta}(y) = 2\tan^{-1}\exp(\alpha\sqrt{3y})$
- Generally soliton lattice. Near the transition, the energy density is

$$\varepsilon = (\frac{2\sqrt{3}\alpha}{\pi} - \beta)n + \frac{8\sqrt{3}}{\pi}n\exp(-\sqrt{3}\pi\alpha/n)$$

- Transition happens when the first term vanishes.

Frank & Van der Merwe (1949)
Bak & Emery (1976)

Commensurate-Incommensurate transition

- Weak-coupling analysis

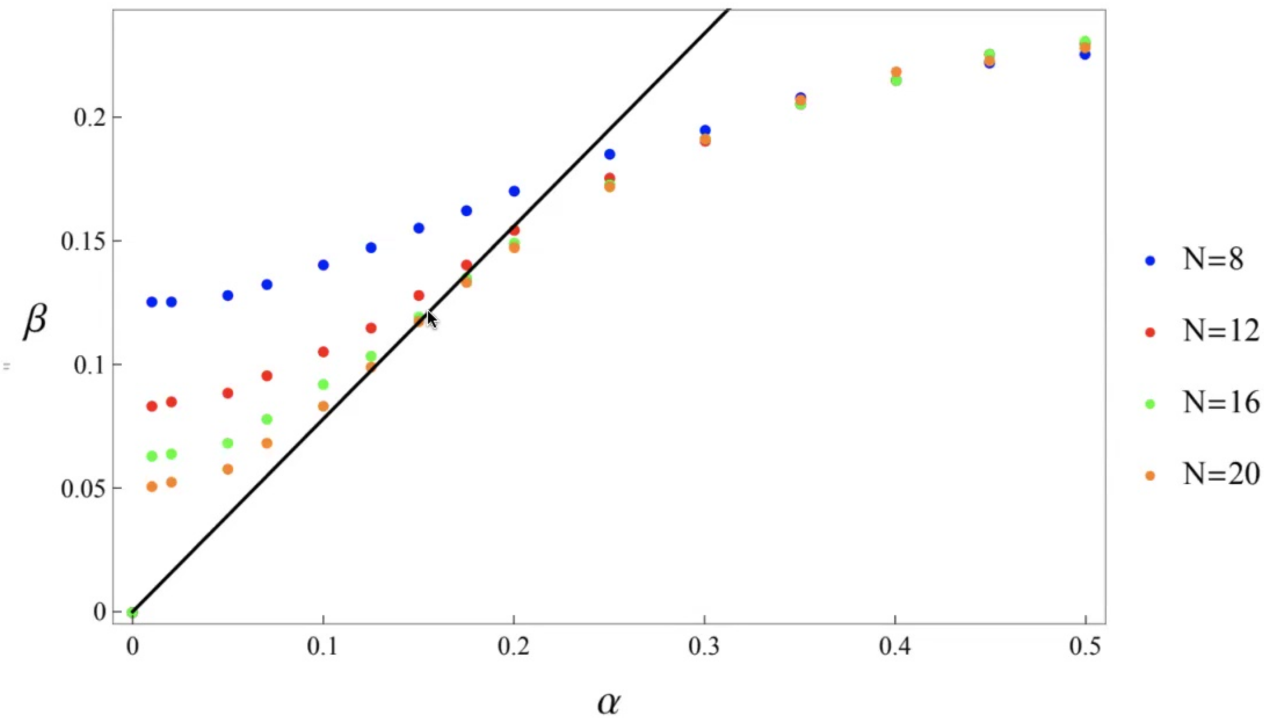

Discussions for this part

- External field stabilizes skyrmions
- The assumption of static AFM layer
- Twisting: increase of d in $\Phi(\boldsymbol{x}) = \sum_i \sin(\boldsymbol{d}_i \cdot \boldsymbol{x})$
- Possible material realization: $MnPS_3$ + Janus TMD

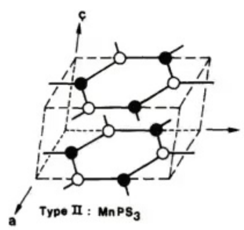

R. Brev, (1986)

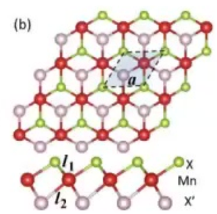

Yuan et al, (2020)

Janus

Outline

- A very rough map
- Moiré magnetism
- Magic continuum in TB square lattice
- *Continuous metal-insulator transition
- Outlook

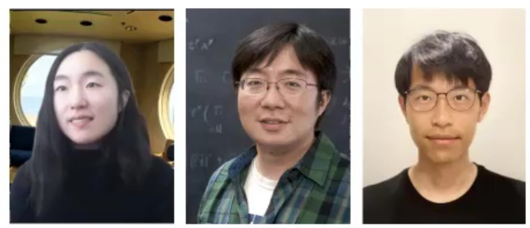

ZXL, Cenke Xu and Chao-Ming Jian, PRB (2021)

Discrete magic angles in TBG

- Exotic physics happens only at discrete magic twisting angles
- Hard to settle into such angles homogeneously
- A magic continuum can make the exotic physics more robust.

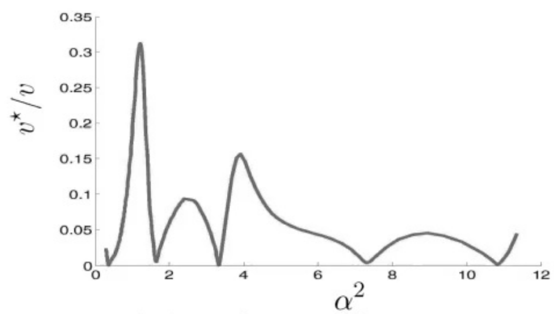

Bistrizer and MacDonald, 2011.

Discrete magic angles in TBG

- Exotic physics happens only at discrete magic twisting angles
- Hard to settle into such angles homogeneously
- A magic continuum can make the exotic physics more robust.

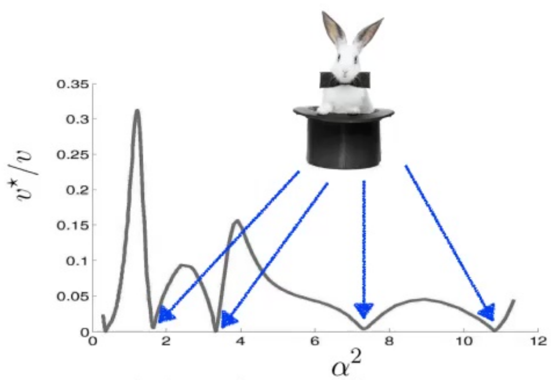

Bistrizer and MacDonald, 2011.

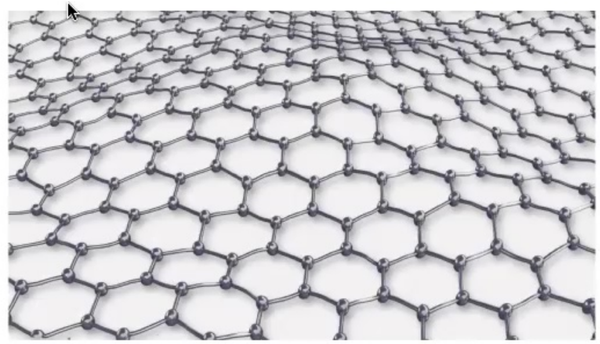

Square lattice with staggered flux I

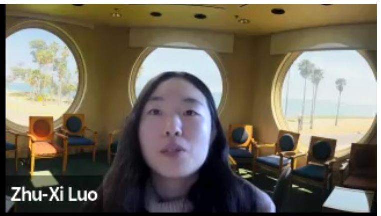

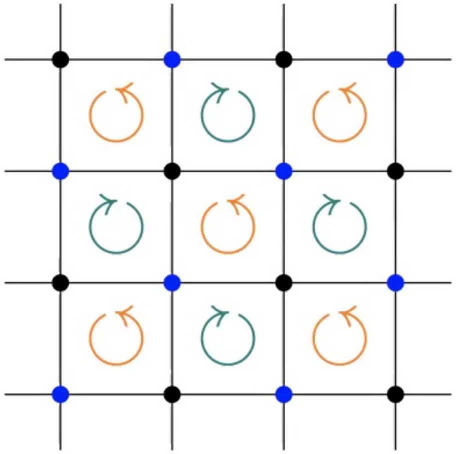

$$H = -\sum_{\boldsymbol{r}\in A}\sum_{\boldsymbol{r}'\in n.n.}[(it + (-1)^{r_y - r'_y}\Delta) f^{\dagger}_{\boldsymbol{r}\alpha} f_{\boldsymbol{r}'\alpha} + h.c.]$$

Apparent breaking of translations

Square lattice with staggered flux I

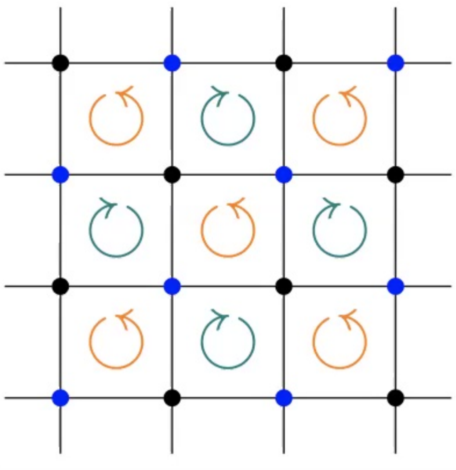

$$H = -\sum_{\boldsymbol{r}\in A}\sum_{\boldsymbol{r}'\in n.n.}[(it + (-1)^{r_y - r'_y}\Delta) f^\dagger_{\boldsymbol{r}\alpha} f_{\boldsymbol{r}'\alpha} + h.c.]$$

Apparent breaking of translations

$$T_x: \quad f_{\boldsymbol{r},\alpha} \to \epsilon_{\boldsymbol{r}} (i\sigma^2)_{\alpha\beta} f^\dagger_{\boldsymbol{r}+\hat{\boldsymbol{x}},\beta},$$
$$T_y: \quad f_{\boldsymbol{r},\alpha} \to \epsilon_{\boldsymbol{r}} (i\sigma^2)_{\alpha\beta} f^\dagger_{\boldsymbol{r}+\hat{\boldsymbol{y}},\beta},$$
$$\mathcal{M}_x: \quad f_{\boldsymbol{r},\alpha} \to f_{\mathcal{M}_x \boldsymbol{r},\alpha},$$
$$R_{\frac{\pi}{2}}: \quad f_{\boldsymbol{r},\alpha} \to \epsilon_{\boldsymbol{r}} f_{R_{\frac{\pi}{2}}\boldsymbol{r},\alpha},$$
$$\mathcal{T}: \quad f_{\boldsymbol{r},\alpha} \to \epsilon_{\boldsymbol{r}} f^\dagger_{\boldsymbol{r},\alpha},$$

Square lattice with staggered flux II

- Initially introduced for d-wave superconductor
- Ansatz for Dirac spin liquid when f's are spinons,

$$\boldsymbol{S}_{\boldsymbol{r}} = \frac{1}{2} f^{\dagger}_{\boldsymbol{r}\alpha} \boldsymbol{\sigma}_{\alpha\beta} f_{\boldsymbol{r}\beta}$$

  parent state for many competing orders.

  Anderson, Affleck, Marston, Wen, Lee, Nagaosa, Rantner, Hermele, Senthil, Fisher, …

- Vulnerable to monopoles

  Karthik & Narayanan; Chester & Pufu; Dyer & Mezei & Pufu; He & Rong & Su…

- We will focus on the case where f's are electrons.

  Hopefully paves the way to twisted bilayers of spin liquids.

Single-layer low-energy physics

- Four flavors of Dirac fermions with SU(4) global symmetry

$$H = \int \frac{d^2\boldsymbol{q}}{(2\pi)^2}\ \psi^\dagger(\boldsymbol{q})(q_1\tau^1 + q_2\tau^2)\psi(\boldsymbol{q})$$

- Add general smooth deformation $\partial \boldsymbol{u} \ll 1$
- Choose Eulerian coordinates $\boldsymbol{x} = \boldsymbol{R} + \boldsymbol{u}(\boldsymbol{x})$.

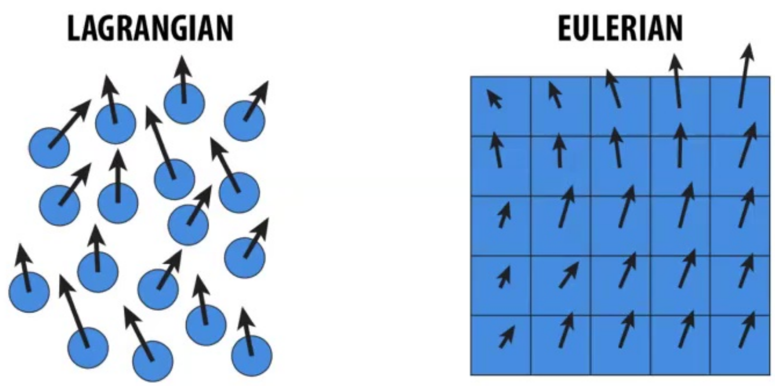

Deformed single layer

- Under this change of basis, Balents, 2019

$$\psi(\boldsymbol{R}) = (1 - \boldsymbol{\nabla} \cdot \boldsymbol{u})^{-1/2} e^{-i\boldsymbol{K}\cdot\boldsymbol{u}} \psi(\boldsymbol{x})$$

$$H_0 = -i \int d^2\boldsymbol{x}\, \psi^\dagger(\boldsymbol{x}) [\tau^i \partial_i + \boxed{\tau^j (\partial_j u^i) \partial_i} - \boxed{i\tau^i K_j \partial_i u^j}] \psi(\boldsymbol{x})$$

Rotation — Shift

- The lattice symmetries now act as

$$\begin{aligned}
T_x &: \quad \psi(\boldsymbol{x}) \to \boxed{e^{2i\boldsymbol{K}\cdot\boldsymbol{u}(\boldsymbol{x})}} \sigma^2 \tau^1 \psi^*(\boldsymbol{x}), \\
T_y &: \quad \psi(\boldsymbol{x}) \to \boxed{e^{2i\boldsymbol{K}\cdot\boldsymbol{u}(\boldsymbol{x})}} (-\sigma^2) \mu^3 \tau^1 \psi^*(\boldsymbol{x}) \\
\mathcal{M}_x &: \quad \psi(\boldsymbol{x}) \to \boxed{e^{i(\boldsymbol{K}' - \boldsymbol{K})\cdot\boldsymbol{u}(\mathcal{M}_x \boldsymbol{x})}} W_1 \psi(\mathcal{M}_x \boldsymbol{x}) \\
R_{\frac{\pi}{2}} &: \quad \psi(\boldsymbol{x}) \to \boxed{e^{i(\boldsymbol{K}'' - \boldsymbol{K})\cdot\boldsymbol{u}(R_{\frac{\pi}{2}} \boldsymbol{x})}} W_2 \psi(R_{\frac{\pi}{2}} \boldsymbol{x}) \\
\mathcal{T} &: \quad \psi(\boldsymbol{x}) \to -\mu^3 \tau^3 \psi^*(\boldsymbol{x}), \quad i \to -i.
\end{aligned}$$

Shift of Dirac cones under deformation

Constraining the interlayer Hamiltonian I

$$H_1 = \int d^2\boldsymbol{x}\ \psi_b^\dagger(\boldsymbol{x}) M[\boldsymbol{u}_t(\boldsymbol{x}), \boldsymbol{u}_b(\boldsymbol{x})]\psi_t(\boldsymbol{x}) + h.c.$$

- Deformation of the bilayer system

$$M[\boldsymbol{u}_t, \boldsymbol{u}_b] = M[\boldsymbol{u}_t - \boldsymbol{u}_b] \equiv M[\boldsymbol{u}]$$

- Deformation of a single layer by lattice constants

$$M[\boldsymbol{u}] = \sum_{\boldsymbol{k}\in(\pi\mathbb{Z},\pi\mathbb{Z})} e^{i\boldsymbol{k}\cdot\boldsymbol{u}} M_{\boldsymbol{k}}$$

- Additional symmetry constraints:

$$T_x: \quad M_{-\boldsymbol{k}-2\boldsymbol{K}} = -\tau^1\sigma^2 M_{\boldsymbol{k}}^* \sigma^2\tau^1,$$
$$T_y: \quad M_{-\boldsymbol{k}-2\boldsymbol{K}} = -\tau^1\mu^3\sigma^2 M_{\boldsymbol{k}}^* \sigma^2\mu^3\tau^1,$$

$$\mathcal{M}_x: \quad M_{\mathcal{M}_x\boldsymbol{k}+\boldsymbol{K}'-\boldsymbol{K}} = W_1^\dagger M_{\boldsymbol{k}} W_1,$$
$$R_{\frac{\pi}{2}}: \quad M_{R_{\frac{\pi}{2}}\boldsymbol{k}+\boldsymbol{K}'-\boldsymbol{K}} = W_2^\dagger M_{\boldsymbol{k}} W_2,$$
$$\mathcal{T}: \quad M_{\boldsymbol{k}} = -\tau^3\mu^3 M_{\boldsymbol{k}}\mu^3\tau^3.$$

Constraining the interlayer Hamiltonian II

- The minimal Fourier expansion:

$$M[\boldsymbol{u}] = 2ie^{-i\boldsymbol{K}\cdot\boldsymbol{u}}[M_0 \sin(\boldsymbol{K}\cdot\boldsymbol{u}) + M_1 \sin(\boldsymbol{K}'\cdot\boldsymbol{u})]$$

$$M_0 = w_1\underline{\tau}^1 + w_2\underline{\mu}^3\tau^1, \quad M_1 = w_1\tau^2 - w_2\mu^3\tau^2$$

Spinor Valley

- Higher moments can be similarly worked out.

- For uniform deformation $\boldsymbol{u} = \hat{\boldsymbol{x}}$, the gapless point splits into four.

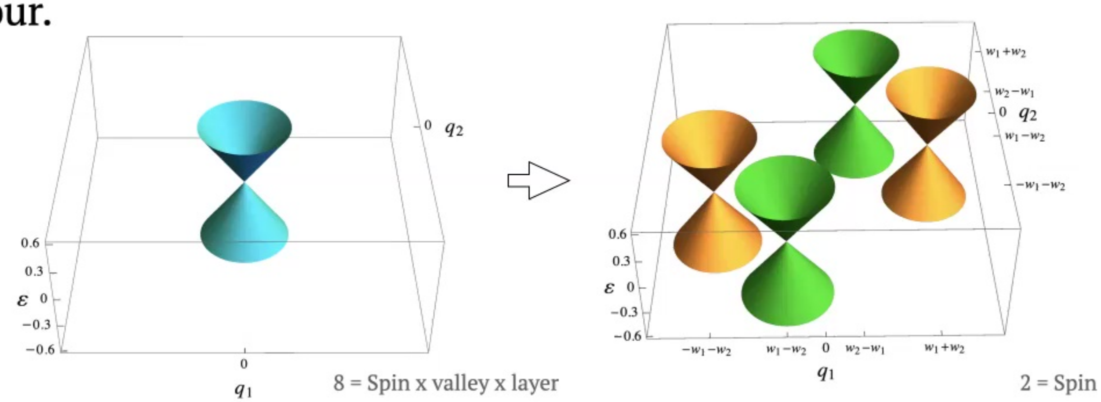

Rigid twist

- For rigid twist, $\boldsymbol{u} = \theta \hat{\boldsymbol{z}} \times \boldsymbol{x}$.

$$H = \int d^2\boldsymbol{x} \Big\{ \sum_{l=t,b} \psi_l^\dagger(\boldsymbol{x})(-i\tau^i \partial_i)\psi_l(\boldsymbol{x}) + \Big(2i\psi_b^\dagger(\boldsymbol{x})(-M_0 \sin x_2 + M_1 \sin x_1)\psi_t(\boldsymbol{x}) + h.c. \Big) \Big\}$$

$$M_0 = w_1\tau^1 + w_2\mu^3\tau^1, \quad M_1 = w_1\tau^2 - w_2\mu^3\tau^2$$

Band flattening, spectrum compression and infinite connectivity

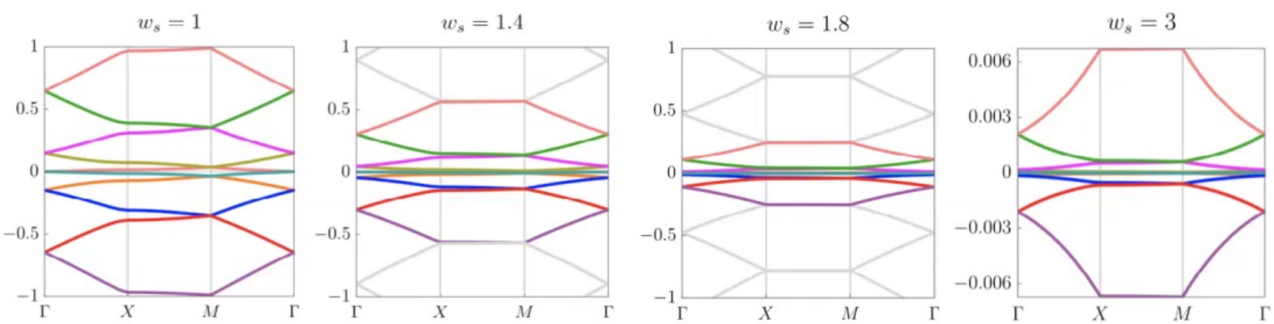

$$w_{s/a} = w_1 \pm w_2$$

Magic continuum

- The Hamiltonian can be rewritten

$$\begin{pmatrix} \psi_t \\ \psi_b \end{pmatrix} = \frac{1}{\sqrt{2}} \begin{pmatrix} \psi \\ is\psi \end{pmatrix} \qquad h = \tau^i(-i\partial_i + A_i)$$

$$A_1 = -2sw_s \sin x_2, \quad A_2 = 2sw_a \sin x_1$$

- The zero-energy states can be exactly solved

$$\psi_+ = c_+ \begin{pmatrix} e^{-B(\boldsymbol{x})} \\ 0 \end{pmatrix}, \quad \psi_- = c_- \begin{pmatrix} 0 \\ e^{B(\boldsymbol{x})} \end{pmatrix}$$

- Treating the q-dependent term as perturbation,

$$h_{\boldsymbol{q}} = \tau^i q_i / I_0(4w_a) I_0(4w_s)$$

Magic continuum

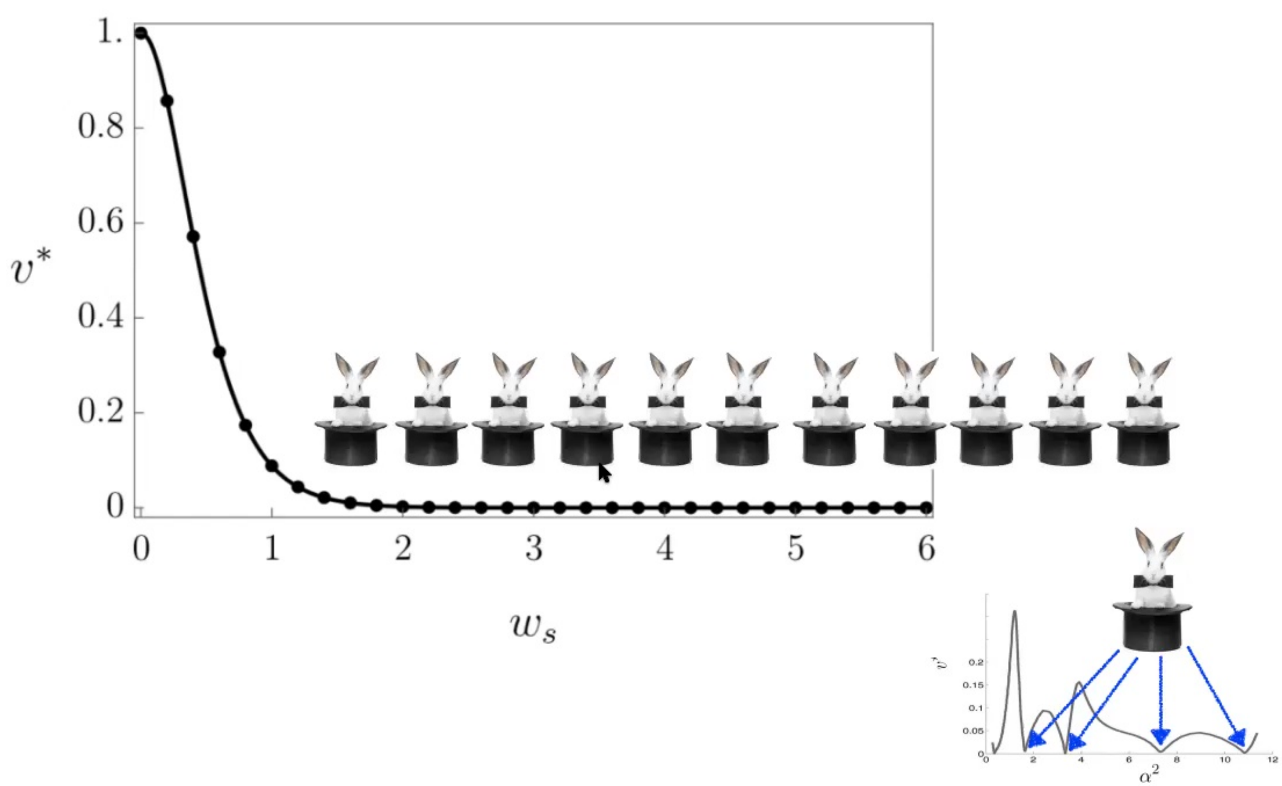

Large number of low-energy minibands

$$B(\boldsymbol{x}) = 2s(w_a \cos x_1 + w_s \cos x_2)$$

- Slowly-varying field, $l_B = 1/\sqrt{B} \ll 1$.
- Landau levels remain a good approximation.
- Degeneracy of 0LL is proportional to the flux.

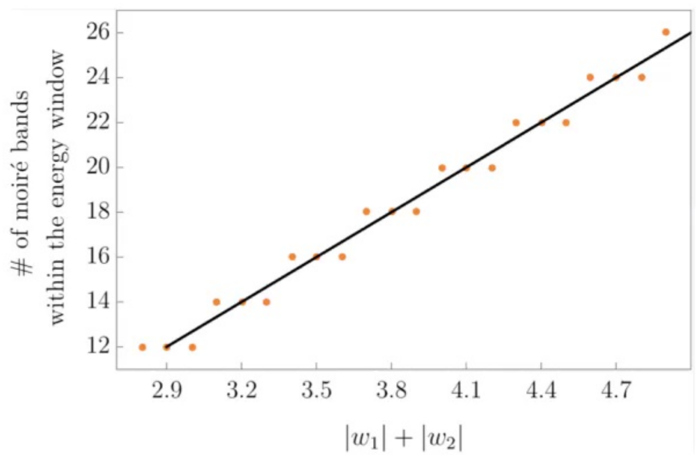

Infinite band connectivity

$$h = \tau^1(-i\partial_1 - 2sw_s \sin x_2) + \tau^2(-i\partial_2 + 2sw_a \sin x_1)$$

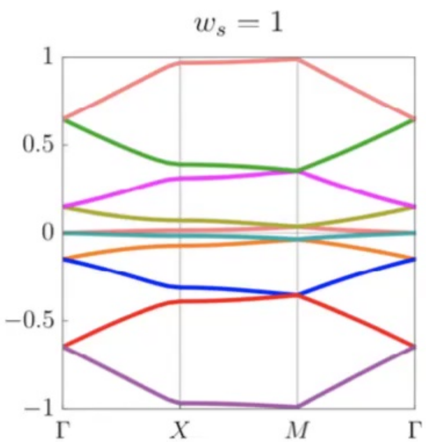

- The total number of Dirac cones must be even for each band.

$$\tilde{R}_\pi \, : \, x_{1,2} \to -x_{1,2} + \pi \, , \;\; \psi(\boldsymbol{x}) \to \psi(\tilde{R}_\pi \boldsymbol{x})$$

$$\tilde{\mathcal{T}} \, : \, \psi(\boldsymbol{x}) \to \tau^1 \psi(\boldsymbol{x}), \;\; i \to -i$$

- Dirac points come in pairs except at the Gamma and M points.

$$R^2_{\frac{\pi}{2}} \, : \, x_{1,2} \to -x_{1,2} \, , \; \psi(\boldsymbol{x}) \to -\tau^z \psi(R^2_{\frac{\pi}{2}} \boldsymbol{x})$$

- So the total number of Dirac cones located at Gamma and M points for each band must be even.

Perfect metal: Mora, Regnault, Bernevig (2019)

Discussion of this part

- Magic continuum
- Spectrum compression
- Infinite connectivity

Discussion of this part

- Magic continuum
- Spectrum compression
- Infinite connectivity

- Lattice dependence?
- Stabilize spin liquid?
- Experiments?

Discussion of this part

Spin-Twisted Optical Lattices: Tunable Flat Bands and Larkin-Ovchinnikov Superfluids

Xi-Wang Luo and Chuanwei Zhang
Phys. Rev. Lett. **126**, 103201 – Published 8 March 2021

Simulating Twistronics without a Twist

Tymoteusz Salamon, Alessio Celi, Ravindra W. Chhajlany, Irénée Frérot, Maciej Lewenstein, Leticia Tarruell, and Debraj Rakshit
Phys. Rev. Lett. **125**, 030504 – Published 14 July 2020

Editors' Suggestion

Cold atoms in twisted-bilayer optical potentials

A. González-Tudela and J. I. Cirac
Phys. Rev. A **100**, 053604 – Published 6 November 2019

Outline

- A very rough map
- Moiré magnetism
- Magic continuum in TB square lattice
- *Continuous metal-insulator transition
- Outlook

Yichen Xu, ZXL Chao-Ming Jian and Cenke Xu, arXiv 2106.14910

Infinite band connectivity

$$h = \tau^1(-i\partial_1 - 2sw_s \sin x_2) + \tau^2(-i\partial_2 + 2sw_a \sin x_1)$$

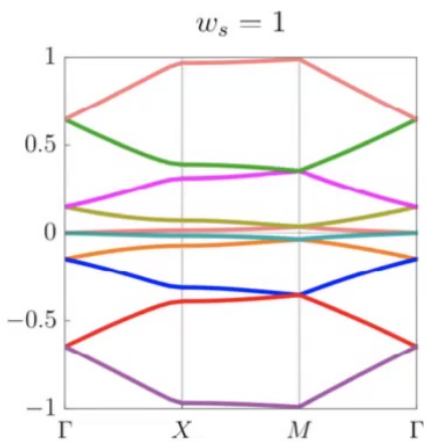

- The total number of Dirac cones must be even for each band.

$$\tilde{R}_\pi \,:\, x_{1,2} \to -x_{1,2} + \pi\,,\;\; \psi(\boldsymbol{x}) \to \psi(\tilde{R}_\pi \boldsymbol{x})$$

$$\tilde{\mathcal{T}} \,:\, \psi(\boldsymbol{x}) \to \tau^1\psi(\boldsymbol{x}),\;\; i \to -i$$

- Dirac points come in pairs except at the Gamma and M points.

$$R^2_{\frac{\pi}{2}} \,:\, x_{1,2} \to -x_{1,2}\,,\;\; \psi(\boldsymbol{x}) \to -\tau^z\psi(R^2_{\frac{\pi}{2}}\boldsymbol{x})$$

- So the total number of Dirac cones located at Gamma and M points for each band must be even.

Perfect metal: Mora, Regnault, Bernevig (2019)

Discussion of this part

- Magic continuum
- Spectrum compression
- Infinite connectivity

Outline

- A very rough map
- Moiré magnetism
- Magic continuum in TB square lattice
- *Continuous metal-insulator transition
- Outlook

Yichen Xu, ZXL Chao-Ming Jian and Cenke Xu, arXiv 2106.14910

Continuous metal-insulator transition

Recent experiments on bilayer TMD

Continuous Mott transition in semiconductor moiré superlattices

Tingxin Li, Shengwei Jiang, Lizhong Li, Yang Zhang, Kaifei Kang, Jiacheng Zhu, Kenji Watanabe, Takashi Taniguchi, Debanjan Chowdhury, Liang Fu, Jie Shan & Kin Fai Mak

Nature **597**, 350–354 (2021) | Cite this article

Features near MIT:

- Bad metal behavior near the transition
- Big jump in resistivity

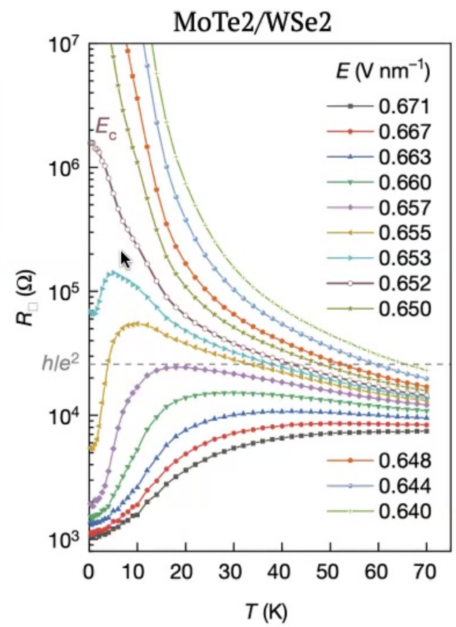

Interaction-driven continuous MIT

- Hubbard model on triangular lattice at half-filling

$$H = \sum_{\boldsymbol{r},\boldsymbol{r}',\alpha} -t_{\boldsymbol{r},\boldsymbol{r}'} c^\dagger_{\boldsymbol{r},\alpha} c_{\boldsymbol{r}',\alpha} + H.c. + \sum_{\boldsymbol{r}} U n_{\boldsymbol{r},\uparrow} n_{\boldsymbol{r},\downarrow} + \cdots$$

Wu, Lovorn, Tutuc, MacDonald (2018).

- Lieb-Shultz-Matthis theorem: the insulating phase cannot be a trivial gapped state preserving translation symmetry.
- Insulating phase breaks translation: two-step transition.
- The insulating phase is a spin liquid with spinon Fermi surface: continuous
  - At MIT, charge dofs are gapped
  - Spins still behave as if there is a ghost Fermi surface

Parton constructions

$$\mathrm{I}: c_{\boldsymbol{r},\alpha} = b_{\boldsymbol{r}} f_{\boldsymbol{r},\alpha}$$

- In I, $\nu_b = 2\nu$, SF/MI transition, one U(1) gauge field a
  - Ioffe-Larkin rule: $\rho = \rho_b + \rho_f$
  - Universal jump: $\Delta\rho = \Delta\rho_b = Rh/e^2$

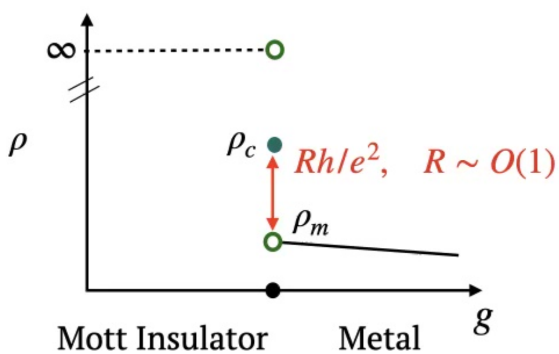

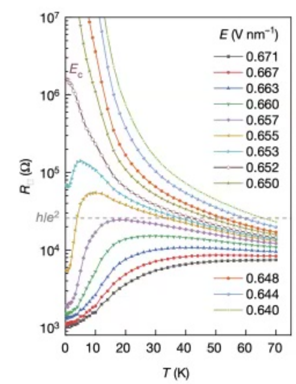

Fisher et al (1990), Cha et al (1991),
Damle and Sachdev (1997),
Lee & Lee, (2005), Senthil, (2008)
...

Parton constructions

$$\mathrm{I} : c_{\boldsymbol{r},\alpha} = b_{\boldsymbol{r}} f_{\boldsymbol{r},\alpha}, \qquad \boxed{\mathrm{II} : c_{\boldsymbol{r},\alpha} = b_{\boldsymbol{r},\alpha} f_{\boldsymbol{r},\alpha}}$$

- Two U(1) gauge fields $a_\uparrow,\ a_\downarrow$
- In II, $\nu_b^\alpha = \nu$, bosons are at half-filling,
- LSM theorem thus says each flavor of boson cannot be a trivial insulator. It's either CDW or topological.
- The bosonic parton further fractionalizes at MIT.

Parton constructions

$$\mathrm{I}: c_{\boldsymbol{r},\alpha} = b_{\boldsymbol{r}} f_{\boldsymbol{r},\alpha}, \quad \boxed{\mathrm{II}: c_{\boldsymbol{r},\alpha} = b_{\boldsymbol{r},\alpha} f_{\boldsymbol{r},\alpha}}$$

Spin-valley locking in TMD

- Two U(1) gauge fields $a_\uparrow,\ a_\downarrow$
- In II, $\nu_b^\alpha = \nu$, bosons are at half-filling,
- LSM theorem thus says each flavor of boson cannot be a trivial insulator. It's either CDW or topological.
- The bosonic parton further fractionalizes at MIT.

Consequence of charge fractionalization

- Each flavor of boson fractionalizes into N parts
- At MIT, charge carrier carries e/N, contributing to resistivity

$$h/e_*^2 \sim N^2 h/e^2$$

- Taking into account all the flavors,

$$\rho_b \sim \frac{N^2 h}{N_b e^2} \equiv \tilde{R}\frac{h}{e^2}$$

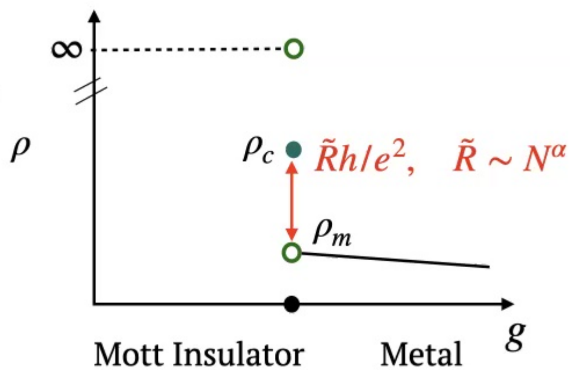

- CDW: $N_b = 2N, \quad \tilde{R} \sim N$
- Z_N topological order: $N_b = 2, \quad \tilde{R} \sim N^2$

Summary

- Moiré magnetism 

- Magic continuum in TB square lattice 

- *Continuous metal-insulator transition

Continuous metal-insulator transition

Recent experiments on bilayer TMD

Continuous Mott transition in semiconductor moiré superlattices

Tingxin Li, Shengwei Jiang, Lizhong Li, Yang Zhang, Kaifei Kang, Jiacheng Zhu, Kenji Watanabe, Takashi Taniguchi, Debanjan Chowdhury, Liang Fu, Jie Shan & Kin Fai Mak

Nature **597**, 350–354 (2021) | Cite this article

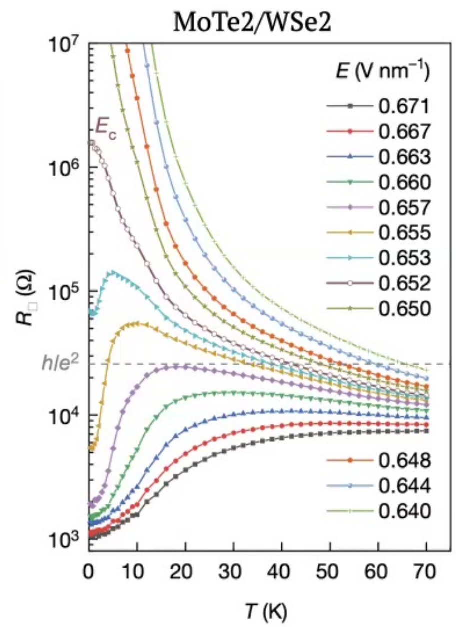

Features near MIT:

- Bad metal behavior near the transition
- Big jump in resistivity

Parton constructions

$$\mathrm{I}: c_{\boldsymbol{r},\alpha} = b_{\boldsymbol{r}} f_{\boldsymbol{r},\alpha}, \qquad \boxed{\mathrm{II}: c_{\boldsymbol{r},\alpha} = b_{\boldsymbol{r},\alpha} f_{\boldsymbol{r},\alpha}}$$

- Two U(1) gauge fields $a_\uparrow,\ a_\downarrow$
- In II, $\nu_b^\alpha = \nu$, bosons are at half-filling,
- LSM theorem thus says each flavor of boson cannot be a trivial insulator. It's either CDW or topological.
- The bosonic parton further fractionalizes at MIT.

Two cases

- CDW: the condensation of a vortex at finite momentum breaks translational symmetry
  - N minima of the vortex band structure, with low energy fields ψ_j Balents et al (2005), Burkov & Balents (2005)

$$\mathcal{L} = \sum_{j=0}^{N-1} (|(\partial_\mu - \mathrm{i}A_\mu)\psi_j|^2 + r|\psi_j|^2) + u(\sum_{j=0}^{N-1} |\psi_j|^2)^2 + \frac{\mathrm{i}}{2\pi} A \wedge d(a + eA_{\mathrm{ext}}) + \cdots$$

- Z_N: N-vortex bound state condensation of b_α at zero momentum

$$\mathcal{L} = |(\partial_\mu - iNA_\mu)\psi|^2 + r|\psi|^2 + u|\psi|^4 + \frac{i}{2\pi} Ad(a + eA_{ext}) + \cdots$$